Structural intensity analysis on irregular shells

Journal of Vibration and Acoustics. Received December 07, 2017;
Accepted manuscript posted July 20, 2018. doi:10.1115/1.4040926

Structural intensity analysis on irregular shells

F. Pires[a,b,1]
[a] Department of Physics,
University of Antwerp,
Groenenborgerlaan 171, 2020 Antwerp, Belgium.
[b] Department of Mechanical Engineering,
Vrije Universiteit Brussel,
Pleinlaan 2, 1050 Brussel, Belgium,
felipe.pires@uantwerpen.be

S. Vanlanduit[a, b]
[a] Department of Electromechanical Engineering,
University of Antwerp,
Groenenborgerlaan 171, 2020 Antwerp, Belgium.
[b] Department of Mechanical Engineering,
Vrije Universiteit Brussel,
Pleinlaan 2, 1050 Brussel, Belgium,
steve.vanlanduit@uantwerpen.be

J.J.J. Dirckx
Department of Physics,
University of Antwerp,
Groenenborgerlaan 171, 2020 Antwerp, Belgium.
joris.dirckx@uantwerpen.be

ABSTRACT

A method is presented to assess the transmission path of vibration energy and to localize sources or sinks on shells with arbitrary shape, constant thickness and isotropic material properties. The derived equations of the structural intensity are based on the Kirchhoff-Love postulates and are formulated in terms of displacements, Lamé parameters, principal curvatures, and their partial derivatives with respect to the principal curvilinear coordinates. To test the accuracy of the method, two numerical models of thin shells with non-uniform curvatures were developed. The coordinates, displacements and principal curvature directions at the shell's outer surface were used to estimate the structural intensity vector fields and the

[1] Corresponding author: felipe.pires@uantwerpen.be

Journal of Vibration and Acoustics. Received December 07, 2017;
Accepted manuscript posted July 20, 2018. doi:10.1115/1.4040926

energy density at the shell's middle surface. The power estimated from the surface integral of the divergence of the structural intensity over the source was compared to the actual power injected in the shell. The absolute error in both models did not exceed 1%, showing that, in theory, the method is able to handle the high-order spatial derivatives of the displacement and geometry data. The qualitative effect of varying the internal damping in the models on the energy transmission was also investigated.

Key words: Structural intensity, injected power, source and sink localization, irregular shells, power flow, variable curvature, principal curvilinear coordinates

1 INTRODUCTION

Structural Intensity (SI) is a powerful concept to study the transmission of vibration energy in plate-like structures. Studies of SI are widely documented in literature; if the structure behaves in accordance with the general theory for thin plates, the SI equations can be directly computed from the sample's a-priori material properties and out-of-plane displacement fields [1–6].

Numerical models were used to investigate SI on structures with a more complex topology: SI was analyzed to investigate the power flow in constituents of locally resonant metamaterials [7, 8], to study the energy flow on offshore platforms to detect cracks under external loads [9], and to investigate the energy paths on stiffened panels [10]. Other heterogeneities have also been addressed, such as the presence of a stepped thickness on plates or the orthotropy of material properties [5,7].

In spite of the continuous progress in this field, the analysis of SI has been mainly applied to structures that satisfy the general theory of thin plates. If the energy transmission is to be assessed on shells, additional terms in the SI equations, related to the in-plane motions at the geometry's middle surface [8–12], cannot be neglected and

Journal of Vibration and Acoustics. Received December 07, 2017;
Accepted manuscript posted July 20, 2018. doi:10.1115/1.4040926

the generalized forces need to be reformulated in accordance with the general theory of thin shells.

The in-plane displacements of the shell's middle surface are uncoupled from the shell's flexural motion [8], which means that all three displacement components at the middle surface are required to determine the SI. However, standard techniques such as laser Doppler vibrometry [13], digital image correlation [14] or holographic interferometry [15] measure displacement fields at the sample's outer surface. The same problem exists with standard shape measurement techniques such as optical profilometry [16].

Another difficulty arises from the curvilinear coordinates of the shell along which the spatial derivatives are calculated. The kinematic equations linking displacements with strains become relatively simple when the principal curvature directions of the shell are chosen as the underlying coordinates [17]. These coordinates are called the Principal Curvilinear Coordinates (PCC) and their directions depend on the shape of the shell being analyzed.

The parametrization of a surface with respect to the PCC is not trivial, as it depends on the shell's shape. So far, the SI on curved shells has been mainly studied on structures whose shape could be parametrized by simple analytical coordinates, such as cylindrical or spherical coordinates [8,18,19].

This work aims to provide a general formulation of SI for shells with arbitrary shape, constant thickness and isotropic material properties. The derived equations are based on the Kirchhoff-love postulates [20] and the principal curvature directions are

Journal of Vibration and Acoustics. Received December 07, 2017;
Accepted manuscript posted July 20, 2018. doi:10.1115/1.4040926

used to parametrize the surface. Moreover, the method is able to calculate the SI from measurements of the displacements and the shape at the outer surface.

The method was tested on numerical models of two different shell structures with non-uniform curvatures. The displacement and shape data of the outer surface were used to recover the vibration energy path at the middle surface. The accuracy of the method was tested by comparing the integrated sources of both models to the actual power being injected to the shells. Finally, the qualitative effect of adding internal damping to the models on the energy transmission was investigated.

2 THEORY

2.1 Differential geometry

2.1.1 Parametrization of a surface

Any surface in a Euclidian space can be represented as a collection of three independent variables, x, y and z. For a surface, these three coordinates can be defined as a function of two independent variables, α and β [21,25]. If there is a one-to-one correspondence between these two sets of coordinates, the position vector $\mathbf{r}$ of the surface can be parametrized as

$$\mathbf{r}(\alpha,\beta) = x(\alpha,\beta)\mathbf{i} + y(\alpha,\beta)\mathbf{j} + z(\alpha,\beta)\mathbf{k}, \tag{1}$$

where α and β are called the curvilinear coordinates of the parametrized surface; $x(\alpha,\beta)$, $y(\alpha,\beta)$ and $z(\alpha,\beta)$ are single-valued and continuous functions of α and β; and $\mathbf{i}$, $\mathbf{j}$ and $\mathbf{k}$ are the standard unit vectors along the x, y and z axis, respectively.

2.1.2 Principal curvatures

Journal of Vibration and Acoustics. Received December 07, 2017;
Accepted manuscript posted July 20, 2018. doi:10.1115/1.4040926

If a given surface is continuous and does not contain any discontinuities in the slope, the normal curvature vector $\mathbf{K_e}$ is defined as [17]:

$$\mathbf{K_e}(\lambda) = K_e(\lambda)\mathbf{e_3}, \tag{2}$$

with K_e the normal curvature and $\mathbf{e_3}$ a unit vector normal to the given surface in a certain point. The parameter λ is associated with all possible planes containing $\mathbf{e_3}$, which intersect the surface along a certain direction in that point. A mathematical description of this parameter is possible by relating the angle of these planes to the parametric coordinates as

$$\lambda = \frac{d\beta}{d\alpha}. \tag{3}$$

From Eqs.(2-3), it can be understood that K_e changes with λ [21]. For every point on the surface, there are two intersecting planes that correspond to the maximum and minimum possible curvatures of the surface in that point. It can be proven that the tangent directions to the surface along these two planes are orthogonal [22]. These particular directions are called the Principal Curvature Directions (PCDs) and are referred to as unit vectors $\mathbf{e_1}$ and $\mathbf{e_2}$. The minimum or maximum curvatures associated with the PCDs are called the principal curvatures K_1 and K_2.

The triad ($\mathbf{e_1}$, $\mathbf{e_2}$, $\mathbf{e_3}$) forms an orthogonal family of unit vectors over any continuous surface. If the parametric coordinates α and β follow the tangent directions $\mathbf{e_1}$ and $\mathbf{e_2}$, respectively, the equations of the theory of thin shells acquire a relatively simple form [17].

Journal of Vibration and Acoustics. Received December 07, 2017;
Accepted manuscript posted July 20, 2018. doi:10.1115/1.4040926

If the increment of α coincides with $\mathbf{e_1}$ and the increment of β with $\mathbf{e_2}$, the parametric coordinates form an orthogonal grid at all points over the surface, which are named the Principal Curvilinear Coordinates (PCCs).

2.1.3 Lamé parameters

The fundamental form parameters [17,23] acquire a simplified form if the PCCs are used as the reference grid of a surface. In this case, the fundamental form parameters are called the Lamé parameters A and B. Their mathematical descriptions are

$$A = \sqrt{x_\alpha^2 + y_\alpha^2 + z_\alpha^2}, \tag{4}$$

$$B = \sqrt{x_\beta^2 + y_\beta^2 + z_\beta^2}. \tag{5}$$

where the subscripts α and β represent partial derivatives with respect to α and β.

The Lamé parameters A and B are related to a change of arc length of the surface caused by a corresponding change of α and β, respectively. Therefore, they can be interpreted as distortion coefficients which transform the change of parametric coordinates into a change of arc length.

Note that the subscripts representing the partial derivatives are extensively used in the equations in this manuscript. For instance, higher-order derivatives are presented by multiple subscripts. E.g., the 2nd order derivative of x with respect to α is denoted by $x_{\alpha\alpha}$.

2.2 General theory of thin shells

Journal of Vibration and Acoustics. Received December 07, 2017;
Accepted manuscript posted July 20, 2018. doi:10.1115/1.4040926

The general linear theory of thin shells is described by three groups of equations: kinematic, equilibrium and constitutive equations. The current work aims to reduce the three-dimensional shell problem to a two-dimensional problem. This is achieved by invoking the Kirchhoff-Love postulates [20], which allow the equilibrium and straining problem to be defined on the shell's middle surface. The equations of the displacements, straining and general internal forces with respect to the orthogonal PCCs are presented below.

2.2.1 Kinematics of shells

From the Kirchhoff assumptions regarding the normal element preservation and the negligible transverse normal stress of the shell, the following relationships can be derived [22]:

$$U^{\gamma} = U + \gamma\vartheta_1, \tag{6}$$

$$V^{\gamma} = V + \gamma\vartheta_2, \tag{7}$$

$$W^{\gamma} = W, \tag{8}$$

$$\vartheta_1 = K_1 U - \frac{1}{A} W_{\alpha}, \tag{9}$$

$$\vartheta_2 = K_2 V - \frac{1}{B} W_{\beta}, \tag{10}$$

where U and V are the in-plane components of the displacement at the middle surface along $\mathbf{e_1}$ and $\mathbf{e_2}$, respectively; W is the out-of-plane displacement along the normal unit vector $\mathbf{e_3}$; ϑ_1 and ϑ_2 are the rotation angles about the tangents to the middle surface (oriented along α and β, respectively); K_1 and K_2 are the principal curvatures along α

Journal of Vibration and Acoustics. Received December 07, 2017;
Accepted manuscript posted July 20, 2018. doi:10.1115/1.4040926

and β, respectively; and γ is the through-thickness coordinate, whose value is zero at the middle surface and bounded by the shell's thickness h, i.e.,

$$-\frac{h}{2} \leq \gamma \leq \frac{h}{2}. \tag{11}$$

The superscript γ in Eqs.(6-8) refers to the dependence of the displacement components on the through-thickness coordinate γ. Note that the displacement W^{γ} has the same value throughout the normal of the middle surface due to the Kirchhoff assumptions.

For a thin shell, the generalized kinematic equations that relate the displacements (U, V and W) with the strain components on the middle surface can be expressed as

$$\varepsilon_1^o = \frac{1}{A}\left(U_\alpha + \frac{A_\beta}{B}V + AK_1W\right), \tag{12}$$

$$\varepsilon_2^o = \frac{1}{B}\left(V_\beta + \frac{B_\alpha}{A}U + BK_2W\right), \tag{13}$$

$$\varepsilon_{12}^o = \frac{1}{AB}\left(BV_\alpha - B_\alpha V + AU_\beta - A_\beta U\right), \tag{14}$$

$$\chi_1 = \frac{1}{A}\left[(\vartheta_1)_\alpha + \frac{A_\beta}{B}\vartheta_2\right], \tag{15}$$

$$\chi_2 = \frac{1}{B}\left[(\vartheta_2)_\beta + \frac{B_\alpha}{A}\vartheta_1\right], \tag{16}$$

$$\chi_{12} = \frac{1}{AB}\left[B(\vartheta_2)_\alpha - B_\alpha\vartheta_2 + A(\vartheta_1)_\beta - A_\beta\vartheta_1\right], \tag{17}$$

Journal of Vibration and Acoustics. Received December 07, 2017;
Accepted manuscript posted July 20, 2018. doi:10.1115/1.4040926

where ε_1^o and ε_2^o are the normal strains; ε_{12}^o is the shear strain, χ_1 and χ_2 are the bending curvatures, and χ_{12} is the torsion of the surface.

2.2.2 Internal forces and moments of a shell

Due to the equilibrium analysis of a 2D element and by integrating the stress resultants and stress couples of a shell over the thickness, one can access the internal forces and moments of an arbitrary shell. These components can be represented as [17,24]:

$$M_1 = D(\chi_1 + \nu\chi_2), \tag{18}$$

$$M_2 = D(\chi_2 + \nu\chi_1), \tag{19}$$

$$M_{12} = M_{21} = \frac{D}{2}(1-\nu)\chi_{12}, \tag{20}$$

$$N_1 = C(\varepsilon_1^o + \nu\varepsilon_2^o), \tag{21}$$

$$N_2 = C[\varepsilon_2^o + \nu\varepsilon_1^o], \tag{22}$$

$$N_{12} = \left[\frac{C}{2}(1-\nu)\varepsilon_{12}^o\right] - M_{12}K_2, \tag{23}$$

$$N_{21} = \left[\frac{C}{2}(1-\nu)\varepsilon_{12}^o\right] - M_{21}K_1, \tag{24}$$

$$D = \frac{\tilde{E}h^3}{12(1-\nu^2)}, \tag{25}$$

$$C = \frac{\tilde{E}h}{(1-\nu^2)}, \tag{26}$$

Journal of Vibration and Acoustics. Received December 07, 2017;
Accepted manuscript posted July 20, 2018. doi:10.1115/1.4040926

$$\tilde{E} = E(1 + \mathrm{j}\eta), \tag{27}$$

$$Q_1 = \frac{1}{AB}\left[2A_\beta M_{12} + B_\alpha(M_1 - M_2) + A(M_{12})_\beta + B(M_1)_\alpha\right], \tag{28}$$

$$Q_2 = \frac{1}{AB}\left[2B_\alpha M_{12} + A_\beta(M_2 - M_1) + B(M_{12})_\alpha + A(M_2)_\beta\right], \tag{29}$$

with M_1 and M_2 the bending moments, M_{12} the twisting moment, N_1 and N_2 the membrane forces, N_{12} the transverse shear force, D the bending rigidity, C the extensional rigidity, E the Young's modulus, ν the Poisson's ratio, η the internal damping loss factor, j the imaginary unit; and Q_1 and Q_2 the transverse shear forces.

2.2.3 Lamé parameters and principal curvatures at the middle surface

The Lamé parameters and principal curvatures vary across the thickness direction of the shell. The relation between these parameters on the middle surface and their corresponding values at any coordinate along the through-thickness direction γ is given by [17],

$$K_d = \frac{K_d^\gamma}{1 - \gamma K_d^\gamma}, \text{for } d = \{1,2\}, \tag{30}$$

$$A = \Pi_1 A^\gamma, \tag{31}$$

$$B = \Pi_2 B^\gamma, \tag{32}$$

$$\Pi_d = \frac{1}{1 + \gamma K_d}, \text{for } d = \{1,2\}. \tag{33}$$

where Π_d is called the curvature coefficient for convenience.

2.3 Structural intensity

Journal of Vibration and Acoustics. Received December 07, 2017;
Accepted manuscript posted July 20, 2018. doi:10.1115/1.4040926

The SI provides the transmission path of vibration energy in a structure, which can be obtained from the vibration velocity and the stress tensor [25]. For shells, the latter two quantities cannot be directly acquired. However, the analysis of SI becomes more convenient when it is formulated in terms of displacement fields. If the shell performs a harmonic motion, the time-averaged SI vector field can be expressed with respect to the PCCs [9] under the Kirchhoff assumptions [24] as follows:

$$\mathbf{I} = I_1\mathbf{e_1} + I_2\mathbf{e_2}, \tag{34}$$

$$I_1 = -(\pi f)\mathrm{Im}\{\tilde{Q}_1\widetilde{W}^* + \widetilde{M}_1\tilde{\vartheta}_1^* + \widetilde{M}_{12}\tilde{\vartheta}_2^* + \widetilde{N}_1\widetilde{U}^* + \widetilde{N}_{12}\tilde{V}^*\}, \tag{35}$$

$$I_2 = -(\pi f)\mathrm{Im}\{\tilde{Q}_2\widetilde{W}^* + \widetilde{M}_2\tilde{\vartheta}_2^* + \widetilde{M}_{21}\tilde{\vartheta}_1^* + \widetilde{N}_2\tilde{V}^* + \widetilde{N}_{21}\widetilde{U}^*\}, \tag{36}$$

where $\mathbf{I}$ represents the active SI vector field per unit length in the frequency domain [W m^{-1}] and $\boldsymbol{f}$ is the frequency at which the structure vibrates. The tilde $\sim$ denotes that the fields are complex and the asterisk $*$ indicates the complex conjugate.

The energy density field [W m^{-2}] of the shell is obtained by applying the divergence operator on the SI (DSI) over the parametrized surface [26]. The DSI can be used to localize regions where the energy path converges (source) or diverges (sink), and can be expressed with respect to the PCCs as

$$\nabla\cdot\mathbf{I} = \frac{1}{AB}\left[(BI_1)_\alpha + (AI_2)_\beta\right] = \frac{B_\alpha}{AB}I_1 + \frac{A_\beta}{AB}I_2 + B(I_1)_\alpha + A(I_2)_\beta. \tag{37}$$

The surface integral of the DSI field over the localized sources or sinks yields the net energy entering or leaving the shell. This parameter is the mean power [W] being transferred to or from the surface and is described with respect to the PCC [27] by:

Journal of Vibration and Acoustics. Received December 07, 2017;
Accepted manuscript posted July 20, 2018. doi:10.1115/1.4040926

$$P = \int [(\nabla \cdot \mathbf{I})AB] d\alpha d\beta. \tag{38}$$

2.3.1 Required inputs for the Structural Intensity analysis on shells

The components involved in the SI formulation (Eq.(34-36)) are the displacements, rotations, internal forces and moments. Eqs.(18-29) and Eqs.(12-17) show that the 6 stress resultants and couples depend on the spatial derivatives of these displacement components, the Lamé parameters and the principal curvatures in the $\alpha\beta$ space. However, since the extraction of the DSI is also a task of the current work, the spatial derivatives are applied to the SI vector components themselves as shown in Eq.(37). The spatial derivative formulations of the SI components (I_1 and I_2), of the 6 stress resultants and couples ($Q_1, Q_2, M_1, M_2, M_{12}, N_1, N_2, N_{12}, N_{21}$), of the strains ($\varepsilon_1^0, \varepsilon_2^0, \varepsilon_{12}^0, \chi_1, \chi_2, \chi_{12}$), rotations ($\vartheta_1, \vartheta_2$), Lamé parameters at the middle and outer surface ($A, B, A^{H/2}, B^{H/2}$) are all shown in the section of supplemental materials as Appendices A to F , respectively. From the equations presented in these Appendices, the highest-order spatial derivatives of each group of the mentioned fields can be identified (they are presented in Table 1). From Table 1, it can be seen that spatial derivatives up to the 3rd or 4th order of the geometrical (A, B, K_1, K_2) and displacement fields (U, V, W) are necessary inputs for the DSI visualization. For the sake of comprehension, the citation of a certain field and all its related spatial derivatives are presented throughout the text by the format

$$\frac{\partial^{m+n}\Phi}{\partial\alpha^m \partial\beta^n}, \tag{39}$$

where $m + n \leq 4$ and $\Phi = \{x, y, z, A, B, K_1, K_2, U, V, W\}$.

Journal of Vibration and Acoustics. Received December 07, 2017;
Accepted manuscript posted July 20, 2018. doi:10.1115/1.4040926

3. MATERIAL AND INPUT DATA

In this method, the SI and DSI were determined on irregular shells by using only information of the sample's outer surface. From Eqs. (18-29, 30-33), it can be noticed that the theory only applies to shells with a constant thickness and isotropic material properties. The only other necessary inputs to determine the SI are the Cartesian coordinates describing the shell's outer surface and the displacement components along these coordinates, i.e., in the directions $\mathbf{i}$, $\mathbf{j}$ and $\mathbf{k}$.

The orientation of the Cartesian coordinates was based on the perspective from which the displacement data were measured. From that "measurement perspective", the x and y axis were aligned with the horizontal and vertical directions of the recorded 2D image, respectively, while the z axis was chosen as the coordinate normal to the xy plane.

All the spatial derivatives of both geometric and displacement fields were entirely processed in the wavenumber domain [28]. The reader is invited to assess detailed explanation on this topic with relation to the SI analysis from the works of [29–31]. The main topic of this article is to present the general equations which depend on the calculation of these derivatives. The subject of the wavenumber processing is not described in this article, since it is far beyond its scope.

The method was tested on two numerical models of a thin shell with a non-uniform curvature and a thickness of 1 mm. Figure 1 presents the two geometries (a rectangular and a circular shell) with corresponding tangent PCDs $\mathbf{e_1}$ and $\mathbf{e_2}$ and mean curvature fields $\left(\frac{K_1+K_2}{2}\right)$. The material properties were based on aluminum: the

Journal of Vibration and Acoustics. Received December 07, 2017;
Accepted manuscript posted July 20, 2018. doi:10.1115/1.4040926

Poisson's coefficient, Young's modulus and density of both samples were set to 0.3; 60 GPa and 2700 kg/m³, respectively.

A localized harmonic pressure load, exciting the structure at 100 Hz, and a viscous damper were included in the models at distinct locations, creating an energy path from the excited surface to the damped surface (Figure 2). The internal damping in the shells was set to zero, so the DSI was zero everywhere outside of the source and sink regions. Afterwards, the energy transmission of these models was compared to a model with an internal damping loss factor of 0.005%.

The coordinates and complex-valued displacements on the upper surface of the shells were exported on a regular grid from the perspective shown in Figure 3. As already mentioned, the x and y coordinates are aligned with the horizontal and vertical directions of this grid, and the z coordinate is directed normal to the xy plane. The displacements at the outer surface defined in this Cartesian coordinate frame are denoted by $\overline{U}$, $\overline{V}$ and $\overline{W}$, and are subsequently represented in the frequency domain.

4. METHODS

The procedure to obtain all the necessary fields for the SI and DSI analysis is divided into two parts (Section 4.1 and Section 4.2). The processing of the geometry (Section 4.1) results in two groups of fields. The first group yields the derivatives of the Lamé parameters $\left(\frac{\partial^{m+n}A}{\partial\alpha^m\partial\beta^n} \text{ and } \frac{\partial^{m+n}B}{\partial\alpha^m\partial\beta^n}\right)$ and principal curvatures $\left(\frac{\partial^{m+n}K_1}{\partial\alpha^m\partial\beta^n} \text{ and } \frac{\partial^{m+n}K_2}{\partial\alpha^m\partial\beta^n}\right)$. The second group provides auxiliary fields that are needed to process the displacements. The processing of the displacements (Section 4.2)

Journal of Vibration and Acoustics. Received December 07, 2017;
Accepted manuscript posted July 20, 2018. doi:10.1115/1.4040926

yields the displacement components at the middle surface with respect to the PCDs $\left(\widetilde{U},\widetilde{V},\widetilde{W}\right)$ and their corresponding spatial derivatives $\left(\frac{\partial^{m+n}\widetilde{U}}{\partial\alpha^m\partial\beta^n},\frac{\partial^{m+n}\widetilde{V}}{\partial\alpha^m\partial\beta^n},\frac{\partial^{m+n}\widetilde{W}}{\partial\alpha^m\partial\beta^n}\right)$. To help the reader to follow this procedure, the processing of the fields in Section (4.1) and Section (4.2) is schematically presented in Figure 4 and Figure 5, respectively. Moreover, figures representing some intermediate steps from both sections can be found in the supplemental material section and are labelled with the letter "S" when referenced in this work. E.g., the first figure from the supplemental material section is labelled as "Figure S1".

4.1 Geometry processing

The goal of this step is to acquire $\frac{\partial^{m+n}A}{\partial\alpha^m\partial\beta^n},\frac{\partial^{m+n}B}{\partial\alpha^m\partial\beta^n},\frac{\partial^{m+n}K_1}{\partial\alpha^m\partial\beta^n}$ and $\frac{\partial^{m+n}K_2}{\partial\alpha^m\partial\beta^n}$ based on the principal curvatures at the outer surface ($K_1^{h/2}$and $K_2^{h/2}$) and the Cartesian coordinates defining that same surface of the shell. Moreover, additional fields are also computed with the sole purpose of assisting the displacement processing step. Part of these fields are the partial derivatives of the x and y coordinates $\frac{\partial^{m+n}x}{\partial\alpha^m\partial\beta^n}$ and $\frac{\partial^{m+n}y}{\partial\alpha^m\partial\beta^n}$, which assist on the change of coordinate domains later on.

The remaining fields are defined here as the Transformation Coefficients (TC) ρ_1,ψ_1,ρ_2 and ψ_2. These coefficients are terms of the PCD which are based on a newly defined triad of unit vector fields $\hat{\mathbf{\imath}},\hat{\mathbf{\jmath}},\hat{\mathbf{k}}$ and whose purpose is clarified next.

4.1.1 Extraction of the Transformation Coefficients

Journal of Vibration and Acoustics. Received December 07, 2017;
Accepted manuscript posted July 20, 2018. doi:10.1115/1.4040926

A non-orthogonal triad of unit vectors $\hat{\mathbf{i}}, \hat{\mathbf{j}}$ and $\hat{\mathbf{k}}$ is introduced to assist the processing of the displacements and are called from now on the Projected Directions (PD). These directions are related to the Cartesian basis by

$$\hat{\mathbf{i}} = q_1\mathbf{i} + s_1\mathbf{k}, \tag{40}$$

$$\hat{\mathbf{j}} = r_2\mathbf{i} + s_2\mathbf{k}, \tag{41}$$

$$\hat{\mathbf{k}} = q_3\mathbf{i} + r_3\mathbf{j} + s_3\mathbf{k}, \tag{42}$$

where $q_1, s_1, r_2, s_2, q_3, r_3$ and s_3 are defined in Appendix G. These vectors are shown in Figure 6 over the circular shell's surface. It can be noted that while the unit vectors $\hat{\mathbf{i}}$ and $\hat{\mathbf{j}}$ are pointing at directions tangent to surface, the $\hat{\mathbf{k}}$ coordinate is the normal component. This representation allows the displacements $\overline{U}$, $\overline{V}$ and $\overline{W}$ to be decomposed into in-plane and out-of-plane displacements. Furthermore, Figure S1 shows that the newly defined tangent vectors $\hat{\mathbf{i}}$ and $\hat{\mathbf{j}}$ can be interpreted as normalized projections of $\mathbf{i}$ and $\mathbf{j}$ if the former vectors are visualized from the projection defined previously (Figure 3). This ensures that, despite projecting $\mathbf{i}$ and $\mathbf{j}$ over the surface, the tangent vector fields $\hat{\mathbf{i}}$ and $\hat{\mathbf{j}}$ are still aligned with the Cartesian coordinates from the perspective view. This newly defined triad of unit vectors makes it possible to process the in-plane displacements over the x and y axis and independent from the shell's shape, as is clarified in Section 4.2.

Both the PDs and PCDs have one unit vector that, respectively, points outward and normal to the geometry's surface ($\hat{\mathbf{k}}$ and $\mathbf{e_3}$, respectively). The remaining vectors

Journal of Vibration and Acoustics. Received December 07, 2017;
Accepted manuscript posted July 20, 2018. doi:10.1115/1.4040926

are tangent to the surface ($\hat{\mathbf{i}}$, $\hat{\mathbf{j}}$, $\mathbf{e_1}$ and $\mathbf{e_2}$), differing only in direction. The PDs and PCDs bases are related by:

$$\mathbf{e_d} = \rho_d \hat{\mathbf{i}} + \psi_d \hat{\mathbf{j}}, \qquad \text{for } d = \{1,2\}, \tag{43}$$

$$\mathbf{e_3} = \hat{\mathbf{k}}, \tag{44}$$

where ρ_d and ψ_d are the TCs defined in Appendix G.

4.1.2 Parametrization

The next step is to relate the independent variables α and β to the x and y coordinates. As previously explained, the parametric coordinates need to be aligned with the PCDs of the outer surface. To complete this step, one first needs to know the principal directions $(\mathbf{e_1}, \mathbf{e_2})$ and respective curvatures $\left(K_1^{h/2}, K_2^{h/2}\right)$ of the surface. Since $\mathbf{e_1}$ and $\mathbf{e_2}$ are orthogonal everywhere on the geometry, α and β must also be orthogonal, so x and y can be treated as functions of α and β, i.e., $x(\alpha, \beta)$ and $y(\alpha, \beta)$.

4.1.3 Partial differentiation on the $\alpha\beta$- space

Initially, the principal curvatures on the outer surface $(K_1^{h/2}, K_2^{h/2})$ and the TCs $(\rho_1, \psi_1, \rho_2, \psi_2)$ are represented on a Cartesian coordinate frame. After parametrization, these fields (including the Cartesian coordinates) are represented on the $\alpha\beta$ space. At this point, the partial derivatives of these fields with respect to α and β can be computed, resulting in the following fields: $\frac{\partial^{m+n} x}{\partial \alpha^m \partial \beta^n}$, $\frac{\partial^{m+n} y}{\partial \alpha^m \partial \beta^n}$, $\frac{\partial^{m+n} z}{\partial \alpha^m \partial \beta^n}$, $\frac{\partial^{m+n} K_1^{h/2}}{\partial \alpha^m \partial \beta^n}$, $\frac{\partial^{m+n} K_2^{h/2}}{\partial \alpha^m \partial \beta^n}$, $\frac{\partial^{m+n} \rho_n}{\partial \alpha^m \partial \beta^n}$ and $\frac{\partial^{m+n} \psi_n}{\partial \alpha^m \partial \beta^n}$. Now that the derivatives of x, y and z with respect to α and β are

Journal of Vibration and Acoustics. Received December 07, 2017;
Accepted manuscript posted July 20, 2018. doi:10.1115/1.4040926

available, Eqs.(4-5, E1-E18) can be used to calculate the derivatives of the Lamé parameters at the outer surface $\left(\frac{\partial^{m+n}A^{h/2}}{\partial\alpha^m\partial\beta^n}\right.$ and $\left.\frac{\partial^{m+n}B^{h/2}}{\partial\alpha^m\partial\beta^n}\right)$.

4.1.4 Lamé parameters and principal curvatures on the middle surface

To determine the derivative fields of the principle curvatures on the middle surface $\left(\frac{\partial^{m+n}K_1}{\partial\alpha^m\partial\beta^n},\frac{\partial^{m+n}K_2}{\partial\alpha^m\partial\beta^n}\right)$, the corresponding fields on the outer surface $\left(\frac{\partial^{m+n}K_1^{h/2}}{\partial\alpha^m\partial\beta^n},\frac{\partial^{m+n}K_2^{h/2}}{\partial\alpha^m\partial\beta^n}\right)$ are substituted into Eq.(30) by using that $\gamma = h/2$.

The extraction of the Lamé parameters on the middle surface $\left(\frac{\partial^{m+n}A}{\partial\alpha^m\partial\beta^n},\frac{\partial^{m+n}B}{\partial\alpha^m\partial\beta^n}\right)$ begins by substituting $\frac{\partial^{m+n}K_1}{\partial\alpha^m\partial\beta^n}$ and $\frac{\partial^{m+n}K_2}{\partial\alpha^m\partial\beta^n}$ into Eqs.(33, F11-F19) to determine the curvature coefficients and their derivatives $\left(\frac{\partial^{m+n}\Pi_1}{\partial\alpha^m\partial\beta^n},\frac{\partial^{m+n}\Pi_2}{\partial\alpha^m\partial\beta^n}\right)$. Then, Φ, Π_d and Φ^* in Eqs.(F1-F10) are respectively substituted by A, Π_1 and $A^{h/2}$; or by B, Π_2 and $B^{h/2}$; resulting in the fields $\frac{\partial^{m+n}A}{\partial\alpha^m\partial\beta^n}$ and $\frac{\partial^{m+n}B}{\partial\alpha^m\partial\beta^n}$. At this point, the only missing data to determine the SI and DSI (Eqs.(34-37)) are the displacement derivatives of the middle surface $\left(\frac{\partial^{m+n}\tilde{U}}{\partial\alpha^m\partial\beta^n},\frac{\partial^{m+n}\tilde{V}}{\partial\alpha^m\partial\beta^n},\frac{\partial^{m+n}\tilde{W}}{\partial\alpha^m\partial\beta^n}\right)$. The next section explains how these fields are calculated from the displacements at the outer surface $(\bar{U},\bar{V},\bar{W})$, the derivative fields of x and y $\left(\frac{\partial^{m+n}x}{\partial\alpha^m\partial\beta^n},\frac{\partial^{m+n}y}{\partial\alpha^m\partial\beta^n}\right)$ and the ones related to the TCs $\left(\frac{\partial^{m+n}\rho_1}{\partial\alpha^m\partial\beta^n},\frac{\partial^{m+n}\psi_1}{\partial\alpha^m\partial\beta^n},\frac{\partial^{m+n}\rho_2}{\partial\alpha^m\partial\beta^n},\frac{\partial^{m+n}\psi_2}{\partial\alpha^m\partial\beta^n}\right)$.

4.2 Displacement processing

This section aims to determine the fields related to the displacements of the shell's middle surface. However, most measurement techniques give only the

Journal of Vibration and Acoustics. Received December 07, 2017;
Accepted manuscript posted July 20, 2018. doi:10.1115/1.4040926

displacements at the structure's outer surface, which are aligned to the standard basis of a Euclidian space $(\mathbf{i}, \mathbf{j}, \mathbf{k})$. The following description shows how these displacement fields can be represented on the PCDs and how their derivatives with respect to the α and β coordinates are obtained.

4.2.1 Separation of in-plane displacements from out-of-plane displacement

First, the displacement fields aligned with the unit vectors $\mathbf{i}$, $\mathbf{j}$ and $\mathbf{k}$ $(\bar{U}, \bar{V}, \bar{W})$ are transformed to the PD representation $(\hat{\mathbf{i}}, \hat{\mathbf{j}}, \hat{\mathbf{k}})$. By doing so, the in-plane and out-of-plane displacements of the outer surface are separated. By using the standard basis to represent the PDs (Eqs.(40-42)), it follows that

$$\hat{U} = q_1\bar{U} + s_1\bar{W}, \tag{45}$$

$$\hat{V} = r_2\bar{V} + s_2\bar{W}, \tag{46}$$

$$\hat{W} = q_3\bar{U} + r_3\bar{V} + s_3\bar{W}. \tag{47}$$

with $\hat{U}$ and $\hat{V}$ the in-plane displacements along $\hat{\mathbf{i}}$ and $\hat{\mathbf{j}}$, respectively; and $\hat{W}$ the out-of-plane displacement along $\hat{\mathbf{k}}$.

As explained in Section (4.1.1), the PDs separate the tangent and normal displacements, but they preserve the continuity of the fields $\hat{U}$, $\hat{V}$ and $\hat{W}$ along the x and y coordinates. This permits their spatial derivatives to be processed conveniently along the Cartesian coordinates, as can be seen in Figure S1. Afterwards, partial derivatives of the in-plane and out-of-plane displacements are calculated up to the 3rd or 4th order along the x and y coordinates $\left(\frac{\partial^{m+n}\hat{U}}{\partial x^m \partial y^n}, \frac{\partial^{m+n}\hat{V}}{\partial x^m \partial y^n}, \frac{\partial^{m+n}\hat{W}}{\partial x^m \partial y^n}\right)$.

Journal of Vibration and Acoustics. Received December 07, 2017;
Accepted manuscript posted July 20, 2018. doi:10.1115/1.4040926

4.2.2 Coordinate transformation

After differentiation of the displacement fields with respect to x and y, the change of coordinate frame of all fields $\left(\frac{\partial^{m+n}\hat{U}}{\partial x^m \partial y^n}, \frac{\partial^{m+n}\hat{V}}{\partial x^m \partial y^n}, \frac{\partial^{m+n}\hat{W}}{\partial x^m \partial y^n}\right)$ can be achieved by treating them as composite functions, i.e., by considering x and y as dependent variables of the $\alpha\beta$-space such that

$$\Phi(x,y) \rightarrow \Phi\big(x(\alpha,\beta), y(\alpha,\beta)\big), \text{for } \Phi = \{\hat{U}, \hat{V}, \hat{W}\}. \tag{48}$$

The chain rule is used to obtain $\frac{\partial^{m+n}\hat{U}}{\partial \alpha^m \partial \beta^n}$, $\frac{\partial^{m+n}\hat{V}}{\partial \alpha^m \partial \beta^n}$ and $\frac{\partial^{m+n}\hat{W}}{\partial \alpha^m \partial \beta^n}$. Applying the chain rule on the 1st order derivatives of a composite function gives

$$\Phi_g = \Phi_x x_g + \Phi_y y_g, \text{for } g = \{\alpha, \beta\}. \tag{49}$$

The components x_α, x_β, y_α and y_β in Eq.(49) were already obtained during the geometry processing (Section (4.1.3)). The fields Φ_x and Φ_y resulted from the previous section (Section (4.2.1)). Since all components on the right-hand side of Eq.(49) are available, the first-order derivatives of the fields $\hat{U}$, $\hat{V}$ and $\hat{W}$ with respect to α and β can be computed.

This process is repeated until all the necessary higher-order derivatives $\left(\frac{\partial^{m+n}\hat{U}}{\partial \alpha^m \partial \beta^n}, \frac{\partial^{m+n}\hat{V}}{\partial \alpha^m \partial \beta^n}, \frac{\partial^{m+n}\hat{W}}{\partial \alpha^m \partial \beta^n}\right)$ are calculated. The equations from which they can be obtained are presented in Appendix H, where the chain rule on a composite function with two independent variables was applied for derivatives up to the fourth order.

4.2.3 Assessment of displacement components on the basis of principal curvature directions

Journal of Vibration and Acoustics. Received December 07, 2017;
Accepted manuscript posted July 20, 2018. doi:10.1115/1.4040926

The next step is to change the basis vectors that represent $\frac{\partial^{m+n}\widehat{U}}{\partial\alpha^m\partial\beta^n}$, $\frac{\partial^{m+n}\widehat{V}}{\partial\alpha^m\partial\beta^n}$ and $\frac{\partial^{m+n}\widehat{W}}{\partial\alpha^m\partial\beta^n}$. The displacement components in the PD basis ($\hat{\mathbf{i}}, \hat{\mathbf{j}}, \hat{\mathbf{k}}$) are changed to the PCD basis ($\mathbf{e_1}, \mathbf{e_2}, \mathbf{e_3}$) by using Eqs.(43-44), yielding the following transformation:

$$\widetilde{U}^{h/2} = \rho_1\widehat{U} + \psi_1\widehat{V}, \tag{50}$$

$$\widetilde{V}^{h/2} = \rho_2\widehat{U} + \psi_2\widehat{V}, \tag{51}$$

$$\widetilde{W}^{h/2} = \widehat{W}, \tag{52}$$

with $\widetilde{U}^{h/2}$ and $\widetilde{V}^{h/2}$ being the in-plane displacements on the outer surface along $\mathbf{e_1}$ and $\mathbf{e_2}$, respectively; and $\widetilde{W}^{h/2}$ the out-of-plane displacement on that surface along $\mathbf{e_3}$. Here, the TCs described in Section (4.1.1) are used to change the basis vectors for the in-plane displacements. Eq.(44) shows that the out-of-plane displacements along $\mathbf{e_3}$ and $\hat{\mathbf{k}}$ are identical, so the spatial derivatives of $\widehat{W}$ and $\widetilde{W}^{h/2}$ are also equal.

This equality does not apply for the in-plane displacements as it is evident from Eqs.(50-51). But since the displacements $\widehat{U}$ and $\widehat{V}$ (described in Section (4.2.1)), and the TCs ρ_d and ψ_d (described in Section (4.1.1)) are available, the fields $\widetilde{U}^{h/2}$ and $\widetilde{V}^{h/2}$ can be assessed. The derivatives of the latter fields are also required for the SI analysis. Their equations are assessable by calculating the derivatives of the right-hand side terms from Eqs.(50-51) and are shown in Appendix I. Since all the right-hand side terms of Eqs.(I3-I11) are also available at this point $\left(\frac{\partial^{m+n}\widehat{U}}{\partial\alpha^m\partial\beta^n}, \frac{\partial^{m+n}\widehat{V}}{\partial\alpha^m\partial\beta^n}, \frac{\partial^{m+n}\widehat{W}}{\partial\alpha^m\partial\beta^n}, \frac{\partial^{m+n}\rho_d}{\partial\alpha^m\partial\beta^n}, \frac{\partial^{m+n}\psi_d}{\partial\alpha^m\partial\beta^n}\right)$, the fields $\frac{\partial^{m+n}\widetilde{U}^{h/2}}{\partial\alpha^m\partial\beta^n}$ and $\frac{\partial^{m+n}\widetilde{V}^{h/2}}{\partial\alpha^m\partial\beta^n}$ can also be computed.

Journal of Vibration and Acoustics. Received December 07, 2017;
Accepted manuscript posted July 20, 2018. doi:10.1115/1.4040926

4.2.4 Assessment of fields related to the middle surface

The final step is to determine the fields at the middle surface. Eq.(8) shows that the out-of-plane displacement has the same value across the thickness direction. Therefore, the fields $\frac{\partial^{m+n}\widetilde{W}}{\partial\alpha^m\partial\beta^n}$ are identical to $\frac{\partial^{m+n}\widetilde{W}^{h/2}}{\partial\alpha^m\partial\beta^n}$.

By isolating the complex-valued fields U and V from Eqs.(6-7), with $\gamma = h/2$, the expressions of the in-plane displacements of the middle surface become

$$\widetilde{U} = \Pi_1 U^*, \tag{53}$$

$$\widetilde{V} = \Pi_2 V^*, \tag{54}$$

$$U^* = \widetilde{U}^{h/2} - \frac{h}{2}\frac{1}{A}\widetilde{W}_\alpha, \tag{55}$$

$$V^* = \widetilde{V}^{h/2} - \frac{h}{2}\frac{1}{B}\widetilde{W}_\beta, \tag{56}$$

All components on the right-hand side of Eqs.(53-56) are available at this point. The derivatives up to the third order of Eqs.(55-56) are presented in Appendix J. The derivatives of Eqs.(53-54) can be obtained from Eqs.(F1-F10) by substituting Φ and Φ^* with $\widetilde{U}$ and U^*, or with $\widetilde{V}$ and V^*, respectively. Once the dynamic behavior at the middle surface has been obtained, Eqs.(34-37) can finally be used to determine the SI and DSI.

5. RESULTS

For the rectangular shell (Figure 1 (a)), the unit vectors ($\mathbf{e_1}$ and $\mathbf{e_2}$) and the tangent PDs ($\hat{\mathbf{i}}$ and $\hat{\mathbf{j}}$) coincide with each other. By using Eq.(43), it becomes clear that this leads to TCs with values of either 1 or 0 over the whole surface of the rectangular shell ($\rho_1 = 1, \psi_1 = 0, \rho_2 = 0$ and $\psi_2 = 1$).

Journal of Vibration and Acoustics. Received December 07, 2017;
Accepted manuscript posted July 20, 2018. doi:10.1115/1.4040926

Because these singular and homogeneous values lead to a simple geometry and displacement processing for the rectangular shell, the processing described in Section (4) is only shown for the circular shell. Lastly, the SI and DSI results of both models are presented.

5.1 Geometry processing

5.1.1 Extraction of the Transformation Coefficients and Parametrization

Since the PCDs of the shells are already known and because the PDs were calculated from Eqs.(40-42), it is possible to compute the four TCs of both geometries. Figure S2 presents the pair of coefficients from the circular shell which are related to $\mathbf{e_1}$, i.e., the coefficients ρ_1 and ψ_1.

As explained previously, the α and β coordinates need to be aligned with the PCDs. The parameterized representations of both geometries are shown in Figure 7. Note that the edge flow of the parametric grid in both geometries are everywhere parallel to the vector fields $\mathbf{e_1}$ and $\mathbf{e_2}$ presented in Figure 1. Furthermore, it is worth noticing that the parametrized grid is orthogonal everywhere on the shells.

5.1.2 Partial differentiation on the $\alpha\beta$- space

After this step, the Cartesian coordinates, principal curvatures at the outer surface and TCs can be transformed and processed on the parametric domain. As an example, Figure 8 (a)-(e)-(i) shows the x coordinate, ρ_1 and $K_1^{h/2}$ of the circular shell on the xy domain. Since the surfaces have already been parametrized, the presented fields can be transformed from the Cartesian frame to the $\alpha\beta$ frame (Figure 8 (b)-(f)-(j)).

Journal of Vibration and Acoustics. Received December 07, 2017;
Accepted manuscript posted July 20, 2018. doi:10.1115/1.4040926

Since these fields can be represented along α and β as a rectangular grid (Figure 8 (b)-(f)-(j)), the spatial derivatives can be performed conveniently. The same figure presents the spatial derivative of the referenced fields with respect to the α coordinate (Figure 8 (c)-(g)-(k)) as an example. The same procedure is repeated until the spatial derivatives up to the 3rd or 4th order of the fields x, y, z, ρ_1, ψ_1, ρ_2 and ψ_2 are obtained. Afterwards, every field is transformed back to the original xy frame (Figure 8 (d)-(h)-(l)). The final procedure of this step is the calculation of the Lamé parameters at the outer surface and their derivatives $\left(\frac{\partial^{m+n}A^{h/2}}{\partial\alpha^m\partial\beta^n},\frac{\partial^{m+n}B^{h/2}}{\partial\alpha^m\partial\beta^n}\right)$ based on the fields related to the Cartesian coordinates $\left(\frac{\partial^{m+n}x}{\partial\alpha^m\partial\beta^n},\frac{\partial^{m+n}y}{\partial\alpha^m\partial\beta^n},\frac{\partial^{m+n}z}{\partial\alpha^m\partial\beta^n}\right)$ (Eqs.(4-5, E1-E18)).

5.1.3 Assessment of the Lamé parameters and Principal curvatures at the middle surface

At this point, the fields related to the principal curvatures $\left(\frac{\partial^{m+n}K_1^{h/2}}{\partial\alpha^m\partial\beta^n},\frac{\partial^{m+n}K_2^{h/2}}{\partial\alpha^m\partial\beta^n}\right)$ and the Lamé parameters $\left(\frac{\partial^{m+n}A^{h/2}}{\partial\alpha^m\partial\beta^n},\frac{\partial^{m+n}B^{h/2}}{\partial\alpha^m\partial\beta^n}\right)$ of the geometry's' outer surface are at hand. By applying Eqs.(30-33, F11-F19, F1-F10) and by substituting γ for $h/2$, the corresponding fields of the middle surface are obtained $\left(\frac{\partial^{m+n}A}{\partial\alpha^m\partial\beta^n},\frac{\partial^{m+n}B}{\partial\alpha^m\partial\beta^n},\frac{\partial^{m+n}K_1}{\partial\alpha^m\partial\beta^n},\frac{\partial^{m+n}K_2}{\partial\alpha^m\partial\beta^n}\right)$.

5.2 Displacement processing

5.2.1 Separation of in-plane displacements from out-of-plane displacement and Coordinate transformation

Journal of Vibration and Acoustics. Received December 07, 2017;
Accepted manuscript posted July 20, 2018. doi:10.1115/1.4040926

The processing of the displacements begins by separating the tangent displacements from the normal displacement. To achieve this, the coefficients of the PDs ($q_1, s_1, r_2, s_2, q_3, r_3$ and s_3) and the displacements of the outer surface ($\bar{U}$, $\bar{V}$ and $\bar{W}$) are inserted in Eqs.(45-47), yielding the in-plane and out-of-plane displacements of the geometry. For the circular shell they are shown in Figure S3.

As explained in Section (4.2.1), this representation is convenient to perform the derivatives along the x and y axis, due to the continuity of the in-plane displacements. Figure S4 shows examples of the displacement field $\hat{V}$ being derived along these axis. This process is repeated up to the third order for the in-plane displacements $\hat{U}$ and $\hat{V}$; and up to the fourth order for the out-of-plane $\widehat{W}$.

The use of the chain rule up to the third and fourth order derivatives is then used to relate the xy and $\alpha\beta$ domain (Eqs.(49, H1-H12)), so the calculated derivatives of the displacement fields are represented with respect to the α and β coordinates. An example of this operation to obtain $\left(\hat{V}\right)_{\alpha}$ is shown in Figure S5.

5.2.2 Assessment of displacement components on the basis of principal curvature directions and related to the middle surface

This section presents the results of the derivatives of the fields described in the $\hat{\mathbf{i}}, \hat{\mathbf{j}}$ and $\hat{\mathbf{k}}$ basis. Since the $\hat{\mathbf{k}}$ direction is identical to $\mathbf{e_3}$ (Eq.(44)), all derivatives of $\widehat{W}$ and $\widetilde{W}^{h/2}$ are equal. The in-plane displacement fields, on the other hand, need to be transformed to the tangent directions $\mathbf{e_1}$ and $\mathbf{e_2}$. Since the fields $\frac{\partial^{m+n}\rho_1}{\partial\alpha^m\partial\beta^n}, \frac{\partial^{m+n}\psi_1}{\partial\alpha^m\partial\beta^n}, \frac{\partial^{m+n}\rho_2}{\partial\alpha^m\partial\beta^n}, \frac{\partial^{m+n}\psi_2}{\partial\alpha^m\partial\beta^n}, \frac{\partial^{m+n}\hat{U}}{\partial\alpha^m\partial\beta^n}$ and $\frac{\partial^{m+n}\hat{V}}{\partial\alpha^m\partial\beta^n}$ are available at this point,

Journal of Vibration and Acoustics. Received December 07, 2017;
Accepted manuscript posted July 20, 2018. doi:10.1115/1.4040926

Eqs.(50-51,I3-I11) can be used to determine $\frac{\partial^{m+n}\widetilde{U}^{h/2}}{\partial\alpha^m\partial\beta^n}$ and $\frac{\partial^{m+n}\widetilde{V}^{h/2}}{\partial\alpha^m\partial\beta^n}$. Figure S6 shows this operation for $\widetilde{U}^{h/2}$ on the circular shell.

The final step is to process $\frac{\partial^{m+n}\widetilde{U}^{h/2}}{\partial\alpha^m\partial\beta^n}$ and $\frac{\partial^{m+n}\widetilde{V}^{h/2}}{\partial\alpha^m\partial\beta^n}$ to obtain the same fields on the shell's middle surface. By using Eqs.(53-56,F1-F19) and by substituting $\gamma = h/2$ in Eqs.(J1-J18), the fields $\frac{\partial^{m+n}\widetilde{U}}{\partial\alpha^m\partial\beta^n}$ and $\frac{\partial^{m+n}\widetilde{V}}{\partial\alpha^m\partial\beta^n}$ can be obtained. As an example, Figure S7 shows the displacement $\widetilde{U}$ on the middle surface of the circular shell compared to the corresponding displacement on the outer surface ($\widetilde{U}^{h/2}$). In addition, the displacements $\widetilde{U}$, $\widetilde{V}$ and $\widetilde{W}$ and their 1st order derivatives with respect to α and β are displayed in Figure S8.

5.3 Structural intensity, net energy and surface integration

At this point, all necessary quantities are available to calculate the SI. By substituting these quantities into the Eqs. (34-36), one can finally visualize the SI taking place on the shell. Figure 9 clearly displays that the energy flows from the region where the source was installed to the region of the damper. Furthermore, by substituting the geometric and displacement data in Eq.(37), the out-of-plane surface power density is obtained. These scalar fields are also shown in Figure 9 for both geometries and display the sources and sinks as concentrated positive and negative values, respectively. Note that no internal damping was included in these cases ($\eta = 0$) and that the DSI is zero everywhere outside of the excited and damped regions.

The next step is to calculate the power from the SI and compare it to the actual injected power. It was explained that the DSI field needs to be integrated on the $\alpha\beta$

Journal of Vibration and Acoustics. Received December 07, 2017;
Accepted manuscript posted July 20, 2018. doi:10.1115/1.4040926

space by using Eq.(38). Figure 10 (a) shows the DSI of the circular shell represented on the xy space, while Figure 10 (b) displays the same field on the $\alpha\beta$ space. This transformation is done on the DSI fields of both geometries, so the surfaces of their respective sources (positive-valued regions) can be integrated by using Eq.(38). Table 2 compares the actual injected power to the ones obtained by taking the surface integral over the sources. The errors of the computed integrations do not exceed 1% for both shells.

Lastly, the analysis was repeated for an internal damping loss factor of 0.005% on both geometries. The resulting energy transmission paths of both shells are visualized in Figure 11. By comparing these results with the ones presented in Figure 9, it can be noticed that the dominant energy paths are similar.

The influence of the internal damping on both models can be perceived by visualizing the SI magnitudes. The magnitudes of the vector fields are high near the sources and gradually decrease towards the sinks.

The effect of adding internal damping can also be noticed by examining the DSI fields in Figure 11. When no damping is present, the energy density on the source and sink are approximately equal in magnitude (see Figure 9). However, when damping is included, the negative density values on the sinks are much less prominent (see Figure 11). This qualitative comparison shows that the power is not only dissipated on the sinks but also on the free zones when a non-zero loss factor is considered.

6. DISCUSSION AND CONCLUSION

Journal of Vibration and Acoustics. Received December 07, 2017;
Accepted manuscript posted July 20, 2018. doi:10.1115/1.4040926

This paper presents a method to calculate the SI, to localize energy sources and sinks, and to assess the transmitted power from shells with non-uniform curvature, constant thickness and isotropic material properties. In addition, this work provides ready-to-use equations for the analysis of the energy transmission, which are based on the Kirchhoff-Love postulates.

The whole process starts with the assumption that the user only has access to displacement and geometry data of the outer surface, i.e., the displacement vector components along the standard unit vectors of the Cartesian space $(\overline{U}, \overline{V}, \overline{W})$, the principal curvature directions and values $\left(\mathbf{e_1}, \mathbf{e_2}, K_1^{h/2} \text{ and } K_2^{h/2}\right)$ and the Cartesian coordinates describing that surface (x, y, z).

The method was tested on two numerical models of a thin shell (a rectangular and a circular thin shell) that both contain a pressure load and a localized damper (to introduce a source and a sink). After processing the geometry fields (the derivatives of the Lamé parameters and principal curvatures), and the displacement fields (needed to recover the mentioned data from the middle surface); clear sources and sinks could be visualized on both samples. Concentrated positive and negative energy density values were found in the exact regions where the pressure load and damper were installed. When no internal damping was introduced in the simulation, the DSI fields were zero on the regions where no external loads were applied.

The difference between the actual injected power and the power calculated from the surface integral over the source showed errors lower than or equal to 1% for both models. This shows that the method can, in theory, provide accurate information

Journal of Vibration and Acoustics. Received December 07, 2017;
Accepted manuscript posted July 20, 2018. doi:10.1115/1.4040926

of the energy transmission path on irregular shells, despite the fact that high-order spatial derivatives of the geometric and displacement fields are needed.

Lastly, the addition of an internal damping loss factor η on both models has also denounced that the energy dissipation takes place not just on the region where the damper was installed but also on the free-zones.

8. ACKNOWLEDGMENT

Financial support was supplied by the Research Foundation of Flanders (FWO), grant No. G049414N.

Journal of Vibration and Acoustics. Received December 07, 2017;
Accepted manuscript posted July 20, 2018. doi:10.1115/1.4040926

NOMENCLATURE

$\mathbf{r}$	Position vector representing a surface in the Euclidian space
(x, y, z)	Cartesian coordinates
(α, β)	Principal Curvilinear coordinates
γ	Through thickness coordinate
$(\mathbf{i}, \mathbf{j}, \mathbf{k})$	Triad of unit vectors from the Euclidian space
$(\hat{\mathbf{i}}, \hat{\mathbf{j}}, \hat{\mathbf{k}})$	Triad of unit vectors from the Projected Directions
$(\mathbf{e_1}, \mathbf{e_2}, \mathbf{e_3})$	Triad of unit vectors from the Principal Curvature Directions
$(\bar{U}, \bar{V}, \bar{W})$	Displacement components from the outer surface along the triad $(\mathbf{i}, \mathbf{j}, \mathbf{k})$
$(\hat{U}, \hat{V}, \hat{W})$	Displacement components from the outer surface along the triad $(\hat{\mathbf{i}}, \hat{\mathbf{j}}, \hat{\mathbf{k}})$
$(U^{h/2}, V^{h/2}, W^{h/2})$	Displacement components from the outer surface along the triad $(\mathbf{e_1}, \mathbf{e_2}, \mathbf{e_3})$
(U, V, W)	Displacement components from the middle surface along the triad $(\mathbf{e_1}, \mathbf{e_2}, \mathbf{e_3})$
$\mathbf{K_e}$	Vector of the normal curvature
λ	Direction of the normal plane intersecting with the surface at one point
K_e	Normal curvature

Journal of Vibration and Acoustics. Received December 07, 2017;
Accepted manuscript posted July 20, 2018. doi:10.1115/1.4040926

K_1, K_2	Principal curvatures
Π_1, Π_2	Curvature coefficients
A, B	Lamé parameters
ϑ_1, ϑ_2	Rotations of tangents to the middle surface
$\varepsilon_1^o, \varepsilon_2^o, \varepsilon_{12}^o$	Normal strains and Shearing strain
$\chi_1, \chi_2, \chi_{12}$	Bending curvatures and Surface torsion
N_1, N_2, N_{12}, N_{21}	Membrane forces and Transverse shear force
M_1, M_2, M_{12}, M_{21}	Bending moments and Twisting moments
Q_1, Q_2	Shear forces
D, C	Bending rigidity and Extensional rigidity
E	Young's modulus
ν	Poisson's coefficient
h	Thickness of the shell
$\mathbf{I}$	Structural intensity vector field
I_1, I_2	Structural intensity vector field components
f	Frequency
P	Transferred mean power
$\rho_1, \psi_1, \rho_2, \psi_2$	Transformation coefficients

Journal of Vibration and Acoustics. Received December 07, 2017;
Accepted manuscript posted July 20, 2018. doi:10.1115/1.4040926

REFERENCES

[1] Semperlotti, F., Conlon, S.C., 2010, "Structural damage identification in plates via nonlinear structural intensity maps," The Journal of the Acoustical Society of America, 127(2), pp. EL48-53. doi:10.1121/1.3290175.

[2] Schmidt, W.T., 2009, "Open-crack Damage Assessments of Aluminum Panels Using Structural Intensity-based Techniques," The Pennsylvania State University. https://etda.libraries.psu.edu/paper/9843/4392.

[3] Arruda, J.R.F., Mas, P., 1998, "Localizing Energy Sources and Sinks in Plates Using Power Flow Maps Computed From Laser Vibrometer Measurements," Shock and Vibration, 5(4), pp. 235–253. doi:10.1155/1998/738387.

[4] Vuye, C., 2011, "Measurement and modeling of sound and vibration fields using a scanning laser Doppler vibrometer," Vrije Universiteit Brussel.

[5] Cho, D., Choi, T., Kim, J., Vladimir, N., 2016, "Structural intensity analysis of stepped thickness rectangular plates utilizing the finite element method," Thin-Walled Structures, 109, pp. 1–12. doi:10.1016/j.tws.2016.09.015.

[6] Roozen, N.B., Guyader, J.L., Glorieux, C., 2015, "Measurement-based determination of the irrotational part of the structural intensity by means of test functional series expansion," Journal of Sound and Vibration, 356, pp. 168–180. doi:10.1016/j.jsv.2015.06.040.

[7] Lamberti, A., Semperlotti, F., 2013, "Detecting closing delaminations in laminated composite plates using nonlinear structural intensity and time reversal mirrors," Smart Materials and Structures, 22(12), pp. 125006. doi:10.1117/12.2009679.

[8] Romano, A.J., Williams, E.G., Abraham, B., Williams, E.G., 1990, "A Poynting vector formulation for thin shells and plates, and its application to structural intensity analysis and source localization. Part I: Theory," The Journal of the Acoustical Society of America, 87(3), pp. 1166–1175. doi:10.1121/1.398790.

[9] Gravic, L., Pavic, G., 1993, "Finite element method for computation of structural intensity by the normal mode approach," Journal of Sound and Vibration, 164(1), pp. 29–43. doi:10.1006/jsvi.1993.1194.

[10] Zhang, Y., 1993, "An experimental method for structural intensity and source location," Iowa State University. doi:10.1016/0191-8141(94)00089-I.

[11] Romano, A.J., Williams, E.G., Russo, K.L., Schuette, L.C., 1992, "On the visualization and analysis of fluid-structure interaction from the perspective of instantaneous intensity," Le Journal de Physique IV, 2(C1), pp. C1-597-C1-600. doi:10.1051/jp4:19921128.

[12] Cho, D.S., Kim, K.S., Kim, B.H., 2010, "Structural intensity analysis of a large container carrier under harmonic excitations of propulsion system," International Journal of Naval Architecture and Ocean Engineering, 2(2), pp. 87–95. doi:10.3744/JNAOE.2010.2.2.087.

[13] Rothberg, S.J., Allen, M.S., Castellini, P., Di Maio, D., Dirckx, J.J.J., Ewins, D.J., Halkon, B.J., Muyshondt, P., Paone, N., Ryan, T., Steger, H., Tomasini, E.P., Vanlanduit, S., Vignola, J.F., 2017, "An international review of laser Doppler

vibrometry: Making light work of vibration measurement," Optics and Lasers in Engineering, 99, pp. 11–22. doi:10.1016/j.optlaseng.2016.10.023.

[14] Schreier, H., Orteu, J.-J., Sutton, M.A., 2009, Image correlation for shape, motion and deformation measurements, Springer, NY, USA.

[15] Pascal, J.-C., Carniel, X., Chalvidan, V., Smigielski, P., 1996, "Determination of phase and magnitude of vibration for energy flow measurements in a plate using holographic interferometry," Optics and Lasers in Engineering, 25, pp. 343–360. doi:10.1016/0143-8166(95)00080-1.

[16] Van der Jeught, S., Dirckx, J.J.J., 2015, "Real-time structured light profilometry: A review," Optics and Lasers in Engineering, 87, pp. 18–31. doi:10.1016/j.optlaseng.2016.01.011.

[17] Ventsel, E., Krauthammer, T., 2001, Thin plates and shells: theory: analysis and applications, CRC press, FL, USA.

[18] Williams, E.G., 1991, "Structural intensity in thin cylindrical shells," The Journal of the Acoustical Society of America, 89(4), pp. 1615-1622. doi:10.1121/1.400996.

[19] Saijyou, K., Yoshikawa, S., 1999, "Structural intensity measurement technique and energy flow of cylindrical influences of shell based on NAH a rib on the acoustic," Journal of the Acoustical Society of Japan, 20(2), pp. 125–136. doi:10.1250/ast.20.125.

[20] Junger, M.C., Feit, D., 1986, Sound, structures, and their interaction, MIT press Cambridge, MA, USA.

[21] Lisle, J., Robinson, M., 1995, "The Mohr circle for curvature and its application to fold description," Journal of Structural Geology, 17(5), pp. 739–750. doi:10.1016/0191-8141(94)00089-I.

[22] Kraus, H., 1967, Thin elastic shells, John Wiley & Sons, NY, USA.

[23] Soedel, W., 2004, Vibrations of shells and plates, CRC Press, FL, USA.

[24] Novozhilov, V.V., 1959, Thin shell theory, P. Noordhoff, Groningen, Netherlands.

[25] Morse, P.M., Feshbach, H., 1946, Methods of theoretical physics, Technology Press.

[26] Boas, M.L., 2006, Mathematical methods in the physical sciences, Wiley.

[27] Hubbard, J.H., Hubbard, B.B., 2015, Vector calculus, linear algebra, and differential forms: a unified approach, Matrix Editions, NY, USA.

[28] Lopes, H.M.R.; Guedes, R. M., Vaz, M.P., 2006, "Techniques in numerical differentiation of experimentally noisy data," 5th International Conference of Mechanical & Materials in Design, Porto, Portugal, pp. 27–28.

[29] Morikawa, R., Ueha, S., Nakamura, K., 1996, "Error evaluation of the structural intensity measured with a scanning laser Doppler vibrometer and a k-space signal processing," The Journal of the Acoustical Society of America, 99(5), pp. 2913–2921. doi:10.1121/1.414878.

[30] Pascal, J.-C., Li, J.-F., Carniel, X., 2002, "Wavenumber Processing Techniques to Determine Structural Intensity and Its Divergence from Optical Measurements without Leakage Effects," Shock and Vibration, 9(1, 2), pp. 57–66. doi:10.1155/2002/850152.

[31] Eck, T., Walsh, S.J., 2012, "Measurement of vibrational energy flow in a plate with

Journal of Vibration and Acoustics. Received December 07, 2017;
Accepted manuscript posted July 20, 2018. doi:10.1115/1.4040926

high energy flow boundary crossing using electronic speckle pattern interferometry," Applied Acoustics, 73(9), pp. 936–951. doi:10.1016/j.apacoust.2012.04.002.

Journal of Vibration and Acoustics. Received December 07, 2017;
Accepted manuscript posted July 20, 2018. doi:10.1115/1.4040926

Figures Caption

Figure 1 – Geometric representation of the shell models from which the SI are determined. Both the rectangular shell (a) and circular shell (b) have a non-uniform curvature as can be noticed from the mean curvature field $\left(\frac{K_1+K_2}{2}\right)$ on their surfaces. The tangent arrows on both geometries show the PCDs $\mathbf{e}_1$ (red arrows) and $\mathbf{e}_2$ (yellow arrows).

Figure 2 – Actual location of the energy sources (red surfaces) and sinks (blue surfaces) on both geometries

Figure 3 – Viewing perspective from which the Cartesian coordinates (x, y, z) and displacement fields $(\overline{U}, \overline{V}, \overline{W})$ at the outer surface were extracted from the rectangular (a) and the circular shell (b)

Figure 4 – Schematic overview of the processing explained in Section (4.1). The fields inside the slashed contours are auxiliary fields and are used as input for the displacement processing (Section (4.2)).

Figure 5 - Schematic overview of the processing explained in Section (4.2)

Figure 6 – Representation of the Projected Directions on the circular shell. Figure (a) represents the tangent vectors $\hat{\imath}$ (red arrows) and $\hat{\jmath}$ (yellow arrows). Figure (b) shows the normal vector $\hat{k}$ (green arrows).

Figure 7 – Representation of the Principal Curvilinear Coordinates α and β as an orthogonal grid on the surfaces of the shells. If the directions of these grids are compared with the Principal Curvature Directions (Figure 1), it can be noticed that both are aligned with each other.

Figure 8 – Processing of the spatial derivatives of the fields x, ρ_1 and $K_1^{h/2}$ of the circular shell. The first (a-e-i) and the second column (b-f-j) show the mentioned fields represented on the xy and the $\alpha\beta$ space, respectively. Afterwards, their spatial derivatives with respect to α and β can be assessed. As an example, the derivatives with respect to α are shown (c-g-k). Finally, the processed fields are transformed back to the original xy space (d-h-l).

Figure 9 – Structural intensity vector field (Eq.(34)) and its respective DSI field (Eq.(37)) for the rectangular (a) and circular shell (b) model.

Figure 10 – DSI field of the circular shell on the xy space (a) and on the αβ space (b). To determine the injected power, Eq.(38) was used to integrate the field defined in Eq.(37) over the source.

Figure 11 – Structural intensity vector field (Eq.(34)) and its corresponding DSI field (Eq.(37)) for the rectangular (a) and circular shell (b) model when an internal damping loss factor of 0.005% was introduced.

Journal of Vibration and Acoustics. Received December 07, 2017;
Accepted manuscript posted July 20, 2018. doi:10.1115/1.4040926

Tables Caption

Table 1 – List of the highest-order spatial derivatives which are needed for the SI and DSI analysis on an irregular shell.

Table 2 – Comparison of the actual injected power (a,b) in both models to the corresponding value that was calculated by surface integration of the DSI over the source (c,d). Note that the highest error does not surpass 1,0% (third column).

Journal of Vibration and Acoustics. Received December 07, 2017;
Accepted manuscript posted July 20, 2018. doi:10.1115/1.4040926

Figures List

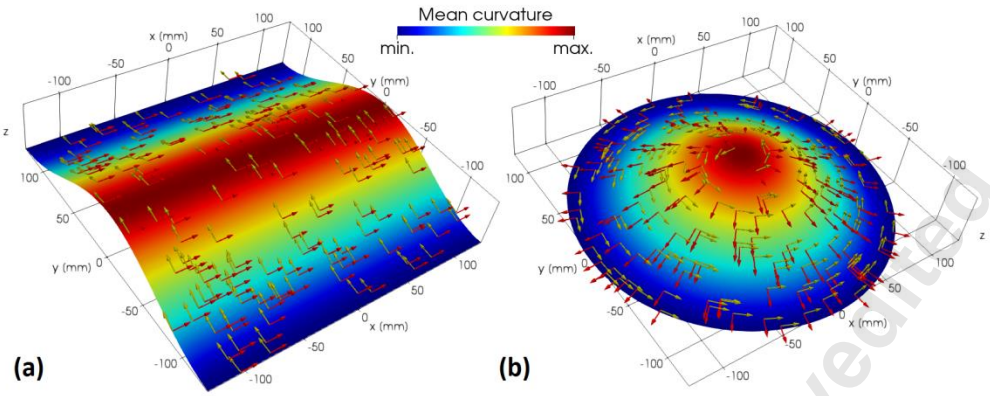

Figure 1 – Geometric representation of the shell models from which the SI are determined. Both the rectangular shell (a) and circular shell (b) have a non-uniform curvature as can be noticed from the mean curvature field $\left(\frac{K_1+K_2}{2}\right)$ on their surfaces. The tangent arrows on both geometries show the PCDs $\mathbf{e}_1$ (red arrows) and $\mathbf{e}_2$ (yellow arrows).

Journal of Vibration and Acoustics. Received December 07, 2017;
Accepted manuscript posted July 20, 2018. doi:10.1115/1.4040926

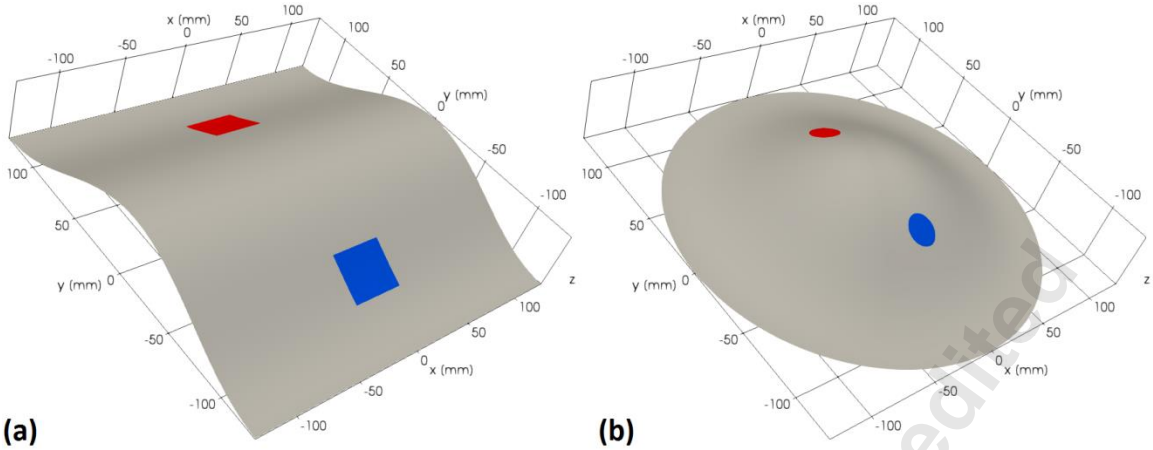

Figure 2 – Actual location of the energy sources (red surfaces) and sinks (blue surfaces) on both geometries

Journal of Vibration and Acoustics. Received December 07, 2017;
Accepted manuscript posted July 20, 2018. doi:10.1115/1.4040926

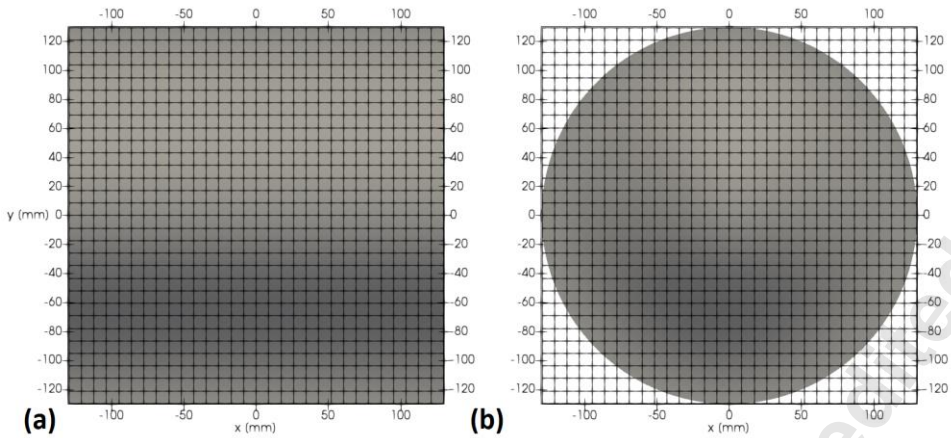

Figure 3 – Viewing perspective from which the Cartesian coordinates (x, y, z) and displacement fields $(\overline{U}, \overline{V}, \overline{W})$ at the outer surface were extracted from the rectangular (a) and the circular shell (b)

Journal of Vibration and Acoustics. Received December 07, 2017;
Accepted manuscript posted July 20, 2018. doi:10.1115/1.4040926

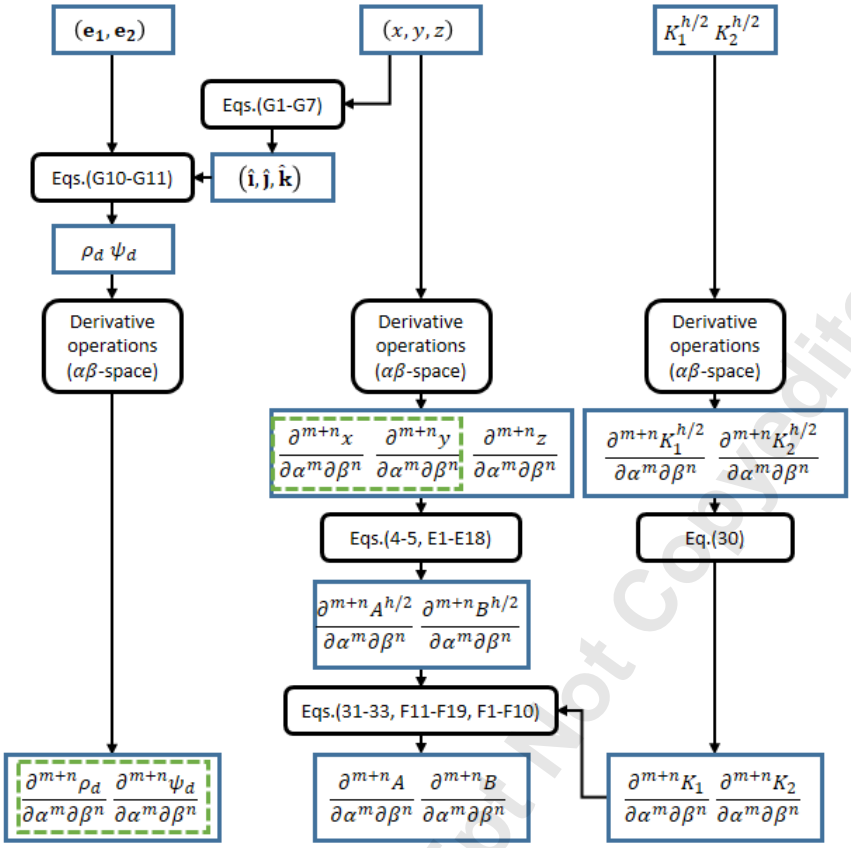

Figure 4 – Schematic overview of the processing explained in Section (4.1). The fields inside the slashed contours are auxiliary fields and are used as input for the displacement processing (Section (4.2)).

Journal of Vibration and Acoustics. Received December 07, 2017;
Accepted manuscript posted July 20, 2018. doi:10.1115/1.4040926

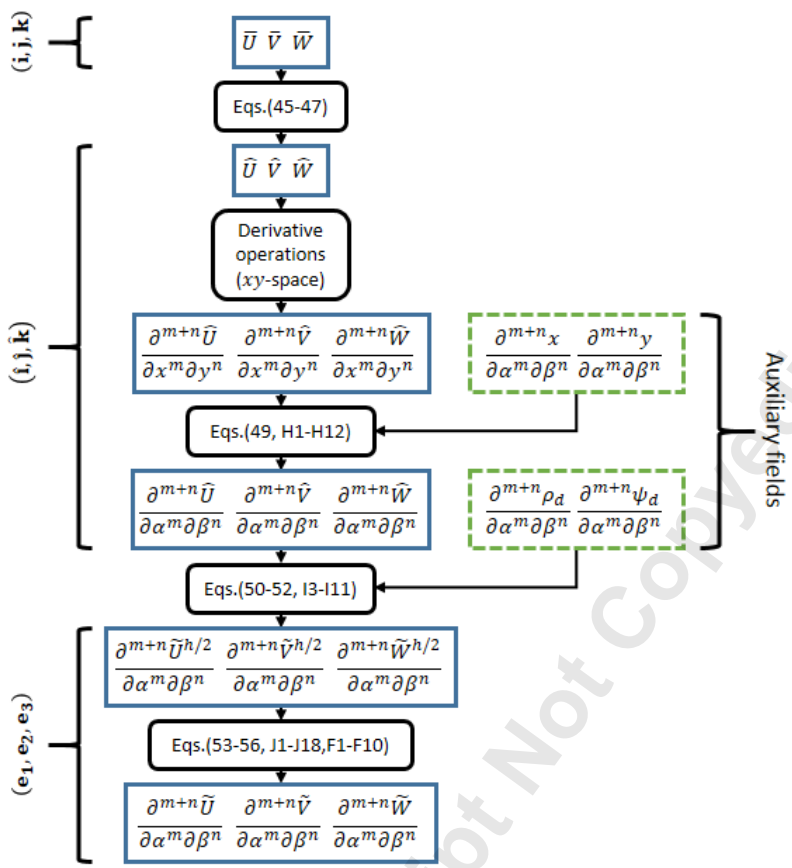

Figure 5 - Schematic overview of the processing explained in Section (4.2)

Journal of Vibration and Acoustics. Received December 07, 2017;
Accepted manuscript posted July 20, 2018. doi:10.1115/1.4040926

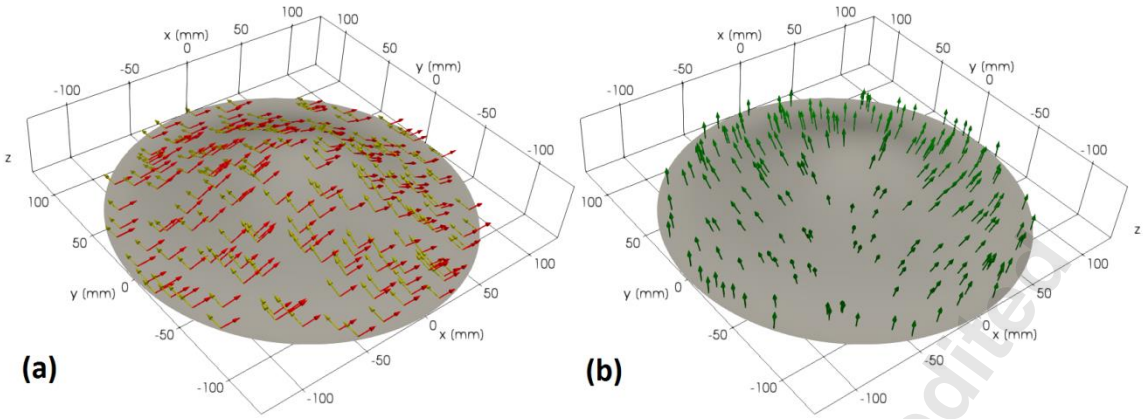

Figure 6 – Representation of the Projected Directions on the circular shell. Figure (a) represents the tangent vectors î (red arrows) and ĵ (yellow arrows). Figure (b) shows the normal vector k̂ (green arrows).

Journal of Vibration and Acoustics. Received December 07, 2017;
Accepted manuscript posted July 20, 2018. doi:10.1115/1.4040926

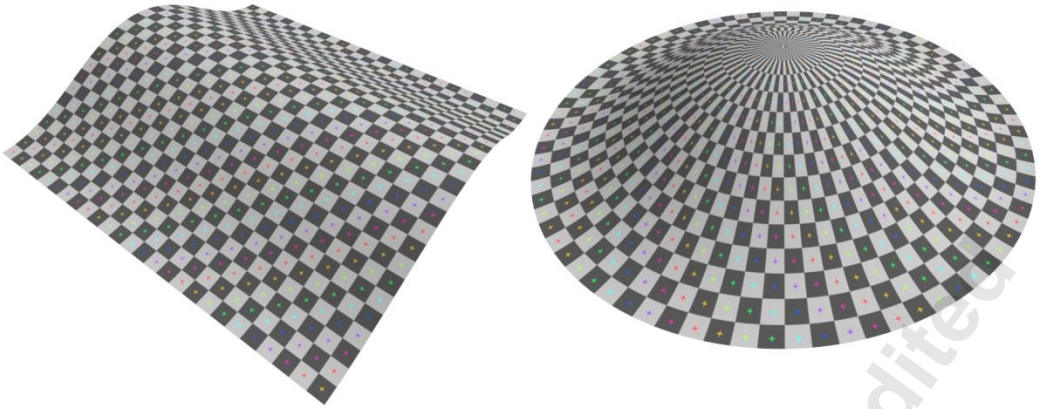

Figure 7 – Representation of the Principal Curvilinear Coordinates α and β as an orthogonal grid on the surfaces of the shells. If the directions of these grids are compared with the Principal Curvature Directions (Figure 1), it can be noticed that both are aligned with each other.

Journal of Vibration and Acoustics. Received December 07, 2017;
Accepted manuscript posted July 20, 2018. doi:10.1115/1.4040926

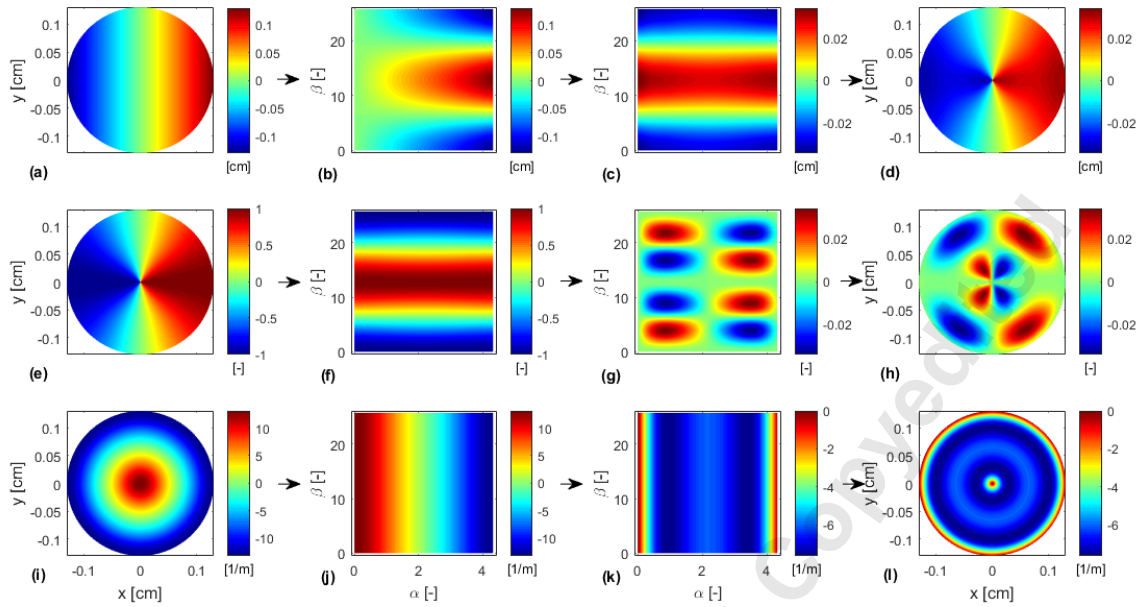

Figure 8 – Processing of the spatial derivatives of the fields x, ρ_1 and $K_1^{h/2}$ of the circular shell. The first (a-e-i) and the second column (b-f-j) show the mentioned fields represented on the xy and the $\alpha\beta$ space, respectively. Afterwards, their spatial derivatives with respect to α and β can be assessed. As an example, the derivatives with respect to α are shown (c-g-k). Finally, the processed fields are transformed back to the original xy space (d-h-l).

Journal of Vibration and Acoustics. Received December 07, 2017;
Accepted manuscript posted July 20, 2018. doi:10.1115/1.4040926

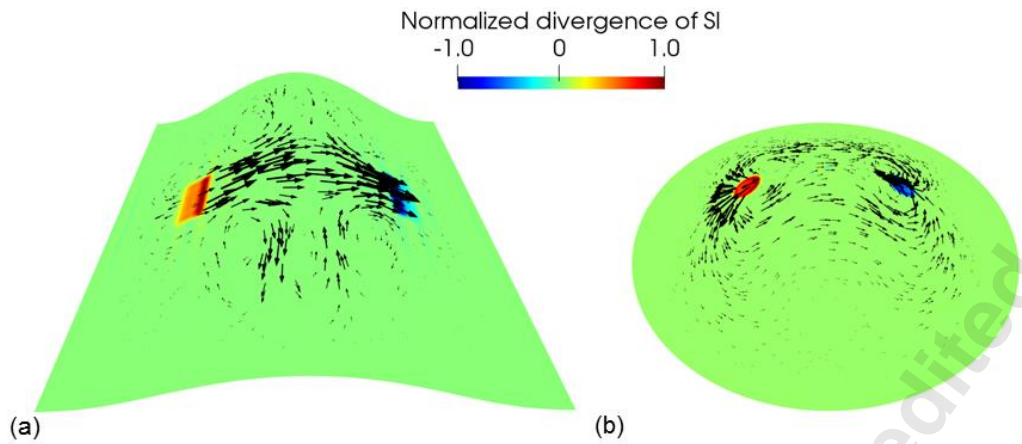

Figure 9 – Structural intensity vector field (Eq.(34)) and its respective DSI field (Eq.(37)) for the rectangular (a) and circular shell (b) model.

Journal of Vibration and Acoustics. Received December 07, 2017;
Accepted manuscript posted July 20, 2018. doi:10.1115/1.4040926

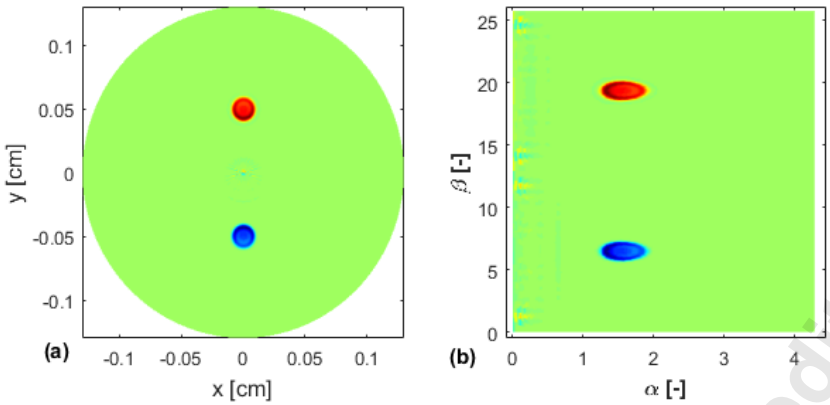

Figure 10 – DSI field of the circular shell on the xy space (a) and on the αβ space (b). To determine the injected power, Eq.(38) was used to integrate the field defined in Eq.(37) over the source.

Journal of Vibration and Acoustics. Received December 07, 2017;
Accepted manuscript posted July 20, 2018. doi:10.1115/1.4040926

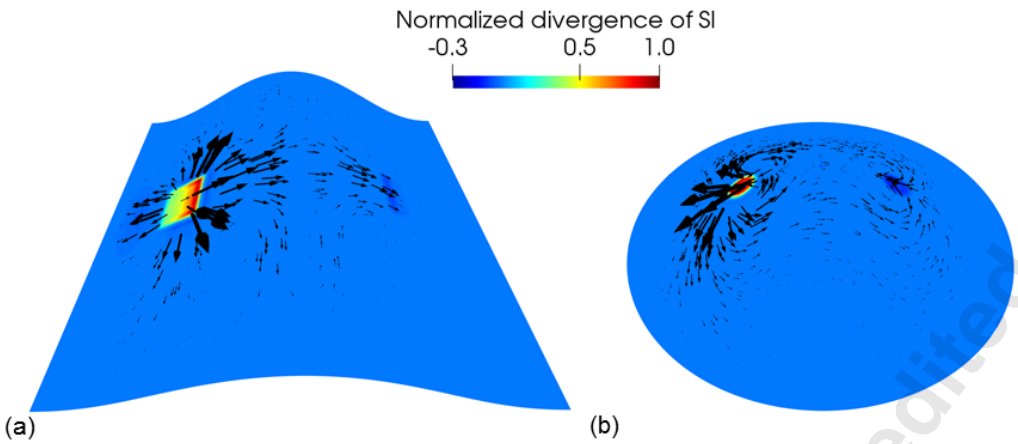

Figure 11 – Structural intensity vector field (Eq.(34)) and its corresponding DSI field (Eq.(37)) for the rectangular (a) and circular shell (b) model when an internal damping loss factor of 0.005% was introduced.

Journal of Vibration and Acoustics. Received December 07, 2017;
Accepted manuscript posted July 20, 2018. doi:10.1115/1.4040926

Tables List

Highest-order spatial derivative	Fields
3rd order $(\Phi_{\alpha\alpha\alpha}, \Phi_{\alpha\alpha\beta}, \Phi_{\alpha\beta\beta}, \Phi_{\beta\beta\beta})$	$\Phi = \{U, V, K_1, K_2, A, B\}$
4th order $(\Phi_{\alpha\alpha\alpha\alpha}, \Phi_{\alpha\alpha\alpha\beta}, \Phi_{\alpha\alpha\beta\beta}, \Phi_{\alpha\beta\beta\beta}, \Phi_{\beta\beta\beta\beta})$	$\Phi = \{W, x, y, z\}$

Table 1 – List of the highest-order spatial derivatives which are needed for the SI and DSI analysis on an irregular shell.

Journal of Vibration and Acoustics. Received December 07, 2017;
Accepted manuscript posted July 20, 2018. doi:10.1115/1.4040926

Membranes	Injected power [W]	Integrated source [W]	Absolute error [%]
Rectangular	$1{,}96 \cdot 10^{-14}$ (a)	$1{,}98 \cdot 10^{-14}$ (c)	0,98
Circular	$1{,}46 \cdot 10^{-15}$ (b)	$1{,}45 \cdot 10^{-15}$ (d)	0,99

Table 2 – Comparison of the actual injected power (a,b) in both models to the corresponding value that was calculated by surface integration of the DSI over the source (c,d). Note that the highest error does not surpass 1,0% (third column).

Journal of Vibration and Acoustics. Received December 07, 2017;
Accepted manuscript posted July 20, 2018. doi:10.1115/1.4040926

SUPPLEMENTAL MATERIAL

APPENDIX A

One group of components of the DSI field presented in Eq.(37) consists of spatial derivatives of the SI vector field components I_1 and I_2. The derivatives of both components are

$$(I_1)_\alpha = -(\pi f)\mathrm{Im}\left\{\left(\tilde{Q}_1\tilde{W}^*\right)_\alpha + \left(\tilde{M}_1\tilde{\vartheta}_1^*\right)_\alpha + \left(\tilde{M}_{12}\tilde{\vartheta}_2^*\right)_\alpha + \left(\tilde{N}_1\tilde{U}^*\right)_\alpha + \left(\tilde{N}_{12}\tilde{V}^*\right)_\alpha\right\}, \tag{A1}$$

$$(I_2)_\beta = -(\pi f)\mathrm{Im}\left\{\left(\tilde{Q}_2\tilde{W}^*\right)_\beta + \left(\tilde{M}_2\tilde{\vartheta}_2^*\right)_\beta + \left(\tilde{M}_{21}\tilde{\vartheta}_1^*\right)_\beta + \left(\tilde{N}_2\tilde{V}^*\right)_\beta + \left(\tilde{N}_{21}\tilde{U}^*\right)_\beta\right\}. \tag{A2}$$

APPENDIX B

It should be stated that all fields related to this work are complex-valued with the exception of the Lamé parameters, Principal Curvatures and the coordinates x, y, z, α and β. Due to the high number of long expressions presented in the appendices and to avoid an excess of symbols, the tilde $\sim$ representing data in the frequency domain was omitted for all variables.

Eqs. (A1-A2) require the 1st order spatial derivatives of the internal forces $(Q_1, Q_2, N_1, N_2, N_{12}, N_{21})$ and moments (M_1, M_2, M_{12}) with respect to α and β. The analytical derivatives of these fields based on Eqs. (18-29) are

$$(Q_1)_\alpha = -\left(\frac{A_\alpha B + AB_\alpha}{AB}Q_1\right) + \frac{1}{AB}\left\{\begin{matrix} B(M_1)_{\alpha\alpha} + A(M_{12})_{\alpha\beta} + B_\alpha[2(M_1)_\alpha - (M_2)_\alpha] + \cdots \\ 2A_\beta(M_{12})_\alpha + A_\alpha(M_{12})_\beta + B_{\alpha\alpha}(M_1 - M_2) + 2A_{\alpha\beta}M_{12} \end{matrix}\right\}, \tag{B1}$$

$$(Q_2)_\beta = -\left(\frac{A_\beta B + AB_\beta}{AB}Q_2\right) + \frac{1}{AB}\left\{\begin{matrix} A(M_2)_{\beta\beta} + B(M_{12})_{\alpha\beta} + A_\beta\left[2(M_2)_\beta - (M_1)_\beta\right] + \cdots \\ 2B_\alpha(M_{12})_\beta + B_\beta(M_{12})_\alpha + A_{\beta\beta}(M_2 - M_1) + 2B_{\alpha\beta}M_{12} \end{matrix}\right\}, \tag{B2}$$

$$(M_1)_\alpha = D[(\chi_1)_\alpha + \nu(\chi_2)_\alpha], \tag{B3}$$

$$(M_1)_\beta = D\left[(\chi_1)_\beta + \nu(\chi_2)_\beta\right], \tag{B4}$$

Journal of Vibration and Acoustics. Received December 07, 2017;
Accepted manuscript posted July 20, 2018. doi:10.1115/1.4040926

$$(M_2)_\alpha = D[(\chi_2)_\alpha + \nu(\chi_1)_\alpha], \tag{B5}$$

$$(M_2)_\beta = D\left[(\chi_2)_\beta + \nu(\chi_1)_\beta\right], \tag{B6}$$

$$(M_{12})_\alpha = \frac{D}{2}(1-\nu)(\chi_{12})_\alpha, \tag{B7}$$

$$(M_{12})_\beta = \frac{D}{2}(1-\nu)(\chi_{12})_\beta, \tag{B8}$$

$$(N_1)_\alpha = C[(\varepsilon_1^o)_\alpha + \nu(\varepsilon_2^o)_\alpha], \tag{B9}$$

$$(N_2)_\beta = C\left[(\varepsilon_2^o)_\beta + \nu(\varepsilon_1^o)_\beta\right], \tag{B10}$$

$$(N_{12})_\alpha = \frac{C}{2}(1-\nu)(\varepsilon_{12}^o)_\alpha - (M_{12})_\alpha K_2 - M_{12}(K_2)_\alpha, \tag{B11}$$

$$(N_{21})_\beta = \frac{C}{2}(1-\nu)(\varepsilon_{12}^o)_\beta - (M_{12})_\beta K_1 - M_{12}(K_2)_\beta. \tag{B12}$$

Eqs. (B1 - B2) contain 2nd order derivatives of the bending and twisting moments. These quantities are obtained by taking the spatial derivatives of Eqs. (B3,B6,B7), yielding

$$(M_1)_{\alpha\alpha} = D[(\chi_1)_{\alpha\alpha} + \nu(\chi_2)_{\alpha\alpha}], \tag{B13}$$

$$(M_2)_{\beta\beta} = D\left[(\chi_2)_{\beta\beta} + \nu(\chi_1)_{\beta\beta}\right], \tag{B14}$$

$$(M_{12})_{\alpha\beta} = \frac{D}{2}(1-\nu)(\chi_{12})_{\alpha\beta}. \tag{B15}$$

APPENDIX C

There are 1st and 2nd order spatial derivatives of the 6 strain components in Eqs. (B3 – B12), which are obtainable from Eqs. (12-17) and are shown below.

$$(\chi_1)_\alpha = \frac{1}{AB}\left[-A_\alpha B\chi_1 + B(\vartheta_1)_{\alpha\alpha} + A_\beta(\vartheta_2)_\alpha + \frac{1}{B}\left(A_{\alpha\beta}B - A_\beta B_\alpha\right)\vartheta_2\right], \tag{C1}$$

$$(\chi_1)_\beta = \frac{1}{AB}\left[-A_\beta B\chi_1 + B(\vartheta_1)_{\alpha\beta} + A_\beta(\vartheta_2)_\beta + \frac{1}{B}\left(A_{\beta\beta}B - A_\beta B_\beta\right)\vartheta_2\right], \tag{C2}$$

Journal of Vibration and Acoustics. Received December 07, 2017;
Accepted manuscript posted July 20, 2018. doi:10.1115/1.4040926

$$(\chi_2)_\alpha = \frac{1}{AB}\left[-AB_\alpha\chi_2 + A(\vartheta_2)_{\alpha\beta} + B_\alpha(\vartheta_1)_\alpha + \frac{1}{A}(AB_{\alpha\alpha} - A_\alpha B_\alpha)\vartheta_2\right], \tag{C3}$$

$$(\chi_2)_\beta = \frac{1}{AB}\left[-AB_\beta\chi_2 + A(\vartheta_2)_{\beta\beta} + B_\alpha(\vartheta_1)_\beta + \frac{1}{A}(AB_{\alpha\beta} - A_\beta B_\alpha)\vartheta_2\right], \tag{C4}$$

$$(\chi_{12})_\alpha = \frac{1}{AB}\begin{bmatrix} -(AB_\alpha + A_\alpha B)\chi_{12} + A(\vartheta_1)_{\alpha\beta} + B(\vartheta_2)_{\alpha\alpha} + \cdots \\ A_\alpha(\vartheta_1)_\beta - A_\beta(\vartheta_1)_\alpha - A_{\alpha\beta}\vartheta_1 - B_{\alpha\alpha}\vartheta_2 \end{bmatrix}, \tag{C5}$$

$$(\chi_{12})_\beta = \frac{1}{AB}\begin{bmatrix} -(AB_\beta + A_\beta B)\chi_{12} + B(\vartheta_2)_{\alpha\beta} + A(\vartheta_1)_{\beta\beta} + \cdots \\ -B_\alpha(\vartheta_2)_\beta + B_\beta(\vartheta_2)_\alpha - B_{\alpha\beta}\vartheta_2 - A_{\beta\beta}\vartheta_1 \end{bmatrix}, \tag{C6}$$

$$(\varepsilon_1^o)_\alpha = \frac{1}{AB}\begin{Bmatrix} -(AB_\alpha + A_\alpha B)\varepsilon_1^o + BU_{\alpha\alpha} + B_\alpha U_\alpha + A_\beta V_\alpha + ABK_1W_\alpha + \cdots \\ A_{\alpha\beta}V + [A_\alpha BK_1 + AB_\alpha K_1 + AB(K_1)_\alpha]W \end{Bmatrix}, \tag{C7}$$

$$(\varepsilon_1^o)_\beta = \frac{1}{AB}\begin{Bmatrix} -(AB_\beta + A_\beta B)\varepsilon_1^o + BU_{\alpha\beta} + B_\beta U_\alpha + A_\beta V_\beta + ABK_1W_\beta + \cdots \\ A_{\beta\beta}V + [A_\beta BK_1 + AB_\beta K_1 + AB(K_1)_\beta]W \end{Bmatrix}, \tag{C8}$$

$$(\varepsilon_2^o)_\alpha = \frac{1}{AB}\begin{Bmatrix} -(AB_\alpha + A_\alpha B)\varepsilon_2^o + AV_{\alpha\beta} + A_\alpha V_\beta + B_\alpha U_\alpha + ABK_2W_\alpha + \cdots \\ B_{\alpha\alpha}U + [A_\alpha BK_2 + AB_\alpha K_2 + AB(K_2)_\alpha]W \end{Bmatrix}, \tag{C9}$$

$$(\varepsilon_2^o)_\beta = \frac{1}{AB}\begin{Bmatrix} -(AB_\beta + A_\beta B)\varepsilon_2^o + AV_{\beta\beta} + A_\beta V_\beta + B_\alpha U_\beta + ABK_2W_\beta + \cdots \\ B_{\alpha\beta}U + [A_\beta BK_2 + AB_\beta K_2 + AB(K_2)_\beta]W \end{Bmatrix}, \tag{C10}$$

$$(\varepsilon_{12}^o)_\alpha = \frac{1}{AB}\begin{bmatrix} -(AB_\alpha + A_\alpha B)\varepsilon_{12}^o + AU_{\alpha\beta} + BV_{\alpha\alpha} + \cdots \\ -A_\beta U_\alpha + A_\alpha U_\beta - A_{\alpha\beta}U - B_{\alpha\alpha}V \end{bmatrix}, \tag{C11}$$

$$(\varepsilon_{12}^o)_\beta = \frac{1}{AB}\begin{bmatrix} -(AB_\beta + A_\beta B)\varepsilon_{12}^o + AU_{\beta\beta} + BV_{\alpha\beta} + \cdots \\ +B_\beta V_\alpha - B_\alpha V_\beta - A_{\beta\beta}U - B_{\alpha\beta}V \end{bmatrix}, \tag{C12}$$

$$(\chi_1)_{\alpha\alpha} = \frac{1}{A}\begin{Bmatrix} -2A_\alpha(\chi_1)_\alpha - A_{\alpha\alpha}\chi_1 + (\vartheta_1)_{\alpha\alpha\alpha} + \cdots \\ \frac{1}{B}\begin{bmatrix} A_\beta(\vartheta_2)_{\alpha\alpha} + 2\left(A_{\alpha\beta} - \frac{A_\beta B_\alpha}{B}\right)(\vartheta_2)_\alpha + \cdots \\ \frac{1}{B}\left(A_{\alpha\alpha\beta}B - 2A_{\alpha\beta}B_\alpha - A_\beta B_{\alpha\alpha} + 2\frac{A_\beta B_\alpha^2}{B}\right)\vartheta_2 \end{bmatrix} \end{Bmatrix}, \tag{C13}$$

$$(\chi_1)_{\beta\beta} = \frac{1}{A}\begin{Bmatrix} -2A_\beta(\chi_1)_\beta - A_{\beta\beta}\chi_1 + (\vartheta_1)_{\alpha\beta\beta} + \cdots \\ \frac{1}{B}\begin{bmatrix} A_\beta(\vartheta_2)_{\beta\beta} + 2\left(A_{\beta\beta} - \frac{A_\beta B_\beta}{B}\right)(\vartheta_2)_\beta + \cdots \\ \frac{1}{B}\left(A_{\beta\beta\beta}B - 2A_{\beta\beta}B_\beta - A_\beta B_{\beta\beta} + 2\frac{A_\beta B_\beta^2}{B}\right)\vartheta_2 \end{bmatrix} \end{Bmatrix}, \tag{C14}$$

$$(\chi_2)_{\alpha\alpha} = \frac{1}{B}\begin{Bmatrix} -2B_\alpha(\chi_2)_\alpha - B_{\alpha\alpha}\chi_2 + (\vartheta_2)_{\alpha\alpha\beta} + \cdots \\ \frac{1}{A}\begin{bmatrix} B_\alpha(\vartheta_1)_{\alpha\alpha} + 2\left(B_{\alpha\alpha} - \frac{A_\alpha B_\alpha}{B}\right)(\vartheta_1)_\alpha + \cdots \\ \frac{1}{A}\left(AB_{\alpha\alpha\alpha} - 2A_\alpha B_{\alpha\alpha} - A_{\alpha\alpha}B_\alpha + 2\frac{A_\alpha^2 B_\alpha}{A}\right)\vartheta_1 \end{bmatrix} \end{Bmatrix}, \tag{C15}$$

Journal of Vibration and Acoustics. Received December 07, 2017;
Accepted manuscript posted July 20, 2018. doi:10.1115/1.4040926

$$(\chi_2)_{\beta\beta} = \frac{1}{B}\begin{Bmatrix} -2B_\beta(\chi_2)_\beta - B_{\beta\beta}\chi_2 + (\vartheta_2)_{\beta\beta\beta} + \cdots \\ \frac{1}{A}\begin{bmatrix} B_\alpha(\vartheta_1)_{\beta\beta} + 2\left(B_{\alpha\beta} - \frac{A_\beta B_\alpha}{B}\right)(\vartheta_1)_\beta + \cdots \\ \frac{1}{A}\left(AB_{\alpha\beta\beta} - 2A_\beta B_{\alpha\beta} - A_{\beta\beta}B_\alpha + 2\frac{A_\beta^2 B_\alpha}{A}\right)\vartheta_1 \end{bmatrix} \end{Bmatrix}, \tag{C16}$$

$$(\chi_{12})_{\alpha\beta} = \frac{1}{AB}\begin{bmatrix} -(AB_\beta + A_\beta B)(\chi_{12})_\alpha - (AB_\alpha + A_\alpha B)(\chi_{12})_\beta + \cdots \\ -(A_{\alpha\beta}B + A_\beta B_\alpha + A_\alpha B_\beta + AB_{\alpha\beta})\chi_{12} + \cdots \\ A(\vartheta_1)_{\alpha\beta\beta} + A_\alpha(\vartheta_1)_{\beta\beta} - A_{\beta\beta}(\vartheta_1)_\alpha - A_{\alpha\beta\beta}\vartheta_2 + \cdots \\ B(\vartheta_2)_{\alpha\alpha\beta} + B_\beta(\vartheta_2)_{\alpha\alpha} - B_{\alpha\alpha}(\vartheta_2)_\beta - B_{\alpha\alpha\beta}\vartheta_2 \end{bmatrix}. \tag{C17}$$

APPENDIX D

The derivatives of the rotations ϑ_1 and ϑ_2 (Eqs. (9 - 10)) from the 1st up to the 3rd order are presented in Eqs. (C1–C6) and (C13–C17). The calculated derivatives of these components are

$$(\vartheta_1)_\alpha = \frac{1}{A}\{-A_\alpha\vartheta_1 + AK_1U_\alpha + [A_\alpha K_1 + A(K_1)_\alpha]U - W_{\alpha\alpha}\}, \tag{D1}$$

$$(\vartheta_1)_\beta = \frac{1}{A}\{-A_\beta\vartheta_1 + AK_1U_\beta + [A_\beta K_1 + A(K_1)_\beta]U - W_{\alpha\beta}\}, \tag{D2}$$

$$(\vartheta_2)_\alpha = \frac{1}{B}[-B_\alpha\vartheta_2 + BK_2V_\alpha + [B_\alpha K_2 + B(K_2)_\alpha]V - W_{\alpha\beta}], \tag{D3}$$

$$(\vartheta_2)_\beta = \frac{1}{B}[-B_\beta\vartheta_2 + BK_2V_\beta + [B_\beta K_2 + B(K_2)_\beta]V - W_{\beta\beta}], \tag{D4}$$

$$(\vartheta_1)_{\alpha\alpha} = \frac{1}{A}\begin{Bmatrix} -2A_\alpha(\vartheta_1)_\alpha - A_{\alpha\alpha}\vartheta_\alpha + AK_1U_{\alpha\alpha} + 2[A_\alpha K_1 + A(K_1)_\alpha]U_\alpha + \cdots \\ [A_{\alpha\alpha}K_1 + 2A_\alpha(K_1)_\alpha + A(K_1)_{\alpha\alpha}]U - W_{\alpha\alpha\alpha} \end{Bmatrix}, \tag{D5}$$

$$(\vartheta_1)_{\alpha\beta} = \frac{1}{A}\begin{Bmatrix} -A_\beta(\vartheta_1)_\alpha - A_{\alpha\beta}\vartheta_1 - A_\alpha(\vartheta_1)_\beta + AK_1U_{\alpha\beta} + \cdots \\ [A_\beta K_1 + A(K_1)_\beta]U_\alpha + \cdots \\ [A_\alpha K_1 + A(K_1)_\alpha]U_\beta + \cdots \\ [A_{\alpha\beta}K_1 + A_\alpha(K_1)_\beta + A_\beta(K_1)_\alpha + A(K_1)_{\alpha\beta}]U - W_{\alpha\alpha\beta} \end{Bmatrix}, \tag{D6}$$

$$(\vartheta_1)_{\beta\beta} = \frac{1}{A}\begin{Bmatrix} -2A_\beta(\vartheta_1)_\beta - A_{\beta\beta}\vartheta_1 + AK_1U_{\beta\beta} + 2[A_\beta K_1 + A(K_1)_\beta]U_\beta + \cdots \\ [A_{\beta\beta}K_1 + 2A_\beta(K_1)_\beta + A(K_1)_{\beta\beta}]U - W_{\alpha\beta\beta} \end{Bmatrix}, \tag{D7}$$

$$(\vartheta_2)_{\alpha\alpha} = \frac{1}{B}\begin{Bmatrix} -2B_\alpha(\vartheta_2)_\alpha - B_{\alpha\alpha}\vartheta_2 + BK_2V_{\alpha\alpha} + 2[B_\alpha K_2 + B(K_2)_\alpha]V_\alpha + \cdots \\ [B_{\alpha\alpha}K_2 + 2B_\alpha(K_2)_\alpha + B(K_2)_{\alpha\alpha}]V - W_{\alpha\alpha\beta} \end{Bmatrix}, \tag{D8}$$

$$(\vartheta_2)_{\alpha\beta} = \frac{1}{B}\begin{Bmatrix} -B_\beta(\vartheta_2)_\alpha - B_{\alpha\beta}\vartheta_2 - B_\alpha(\vartheta_2)_\beta + [B_\beta K_2 + B(K_2)_\beta]V_\alpha + \cdots \\ BK_2V_{\alpha\beta} + [B_\alpha K_2 + B(K_2)_\alpha]V_\beta + \cdots \\ [B_{\alpha\beta}K_2 + B_\alpha(K_2)_\beta + B_\beta(K_2)_\alpha + B(K_2)_{\alpha\beta}]V - W_{\alpha\beta\beta} \end{Bmatrix}, \tag{D9}$$

Journal of Vibration and Acoustics. Received December 07, 2017;
Accepted manuscript posted July 20, 2018. doi:10.1115/1.4040926

$$(\vartheta_2)_{\beta\beta} = \frac{1}{B}\begin{Bmatrix} -2B_\beta(\vartheta_2)_\beta - B_{\beta\beta}\vartheta_2 + BK_2V_{\beta\beta} + 2\left[B_\beta K_2 + B(K_2)_\beta\right]V_\beta + \cdots \\ \left[B_{\beta\beta}K_2 + 2B_\beta(K_2)_\beta + B(K_2)_{\beta\beta}\right]V - W_{\beta\beta\beta} \end{Bmatrix}, \tag{D10}$$

$$(\vartheta_1)_{\alpha\alpha\alpha} = \frac{1}{A}\begin{Bmatrix} -3A_\alpha(\vartheta_1)_{\alpha\alpha} - 3A_{\alpha\alpha}(\vartheta_1)_\alpha - A_{\alpha\alpha\alpha}\vartheta_1 + \cdots \\ AK_1U_{\alpha\alpha\alpha} + 3[A_\alpha K_1 + A(K_1)_\alpha]U_{\alpha\alpha} + \cdots \\ 3[A_{\alpha\alpha}K_1 + 2A_\alpha(K_1)_\alpha + A(K_1)_{\alpha\alpha}]U_\alpha + \cdots \\ [A_{\alpha\alpha\alpha}K_1 + 3A_{\alpha\alpha}(K_1)_\alpha + 3A_\alpha(K_1)_{\alpha\alpha} + A(K_1)_{\alpha\alpha\alpha}]U - W_{\alpha\alpha\alpha\alpha} \end{Bmatrix}, \tag{D11}$$

$$(\vartheta_1)_{\alpha\beta\beta} = \frac{1}{A}\begin{Bmatrix} -2A_\beta(\vartheta_1)_{\alpha\beta} - A_\alpha(\vartheta_1)_{\beta\beta} - A_{\beta\beta}(\vartheta_1)_\alpha - 2A_{\alpha\beta}(\vartheta_1)_\beta - A_{\alpha\beta\beta}\vartheta_1 + \cdots \\ AK_1U_{\alpha\beta\beta} + 2\left[A_\beta K_1 + A(K_1)_\beta\right]U_{\alpha\beta} + [A_\alpha K_1 + A(K_1)_\alpha]U_{\beta\beta} + \cdots \\ \left[A_{\beta\beta}K_1 + 2A_\beta(K_1)_\beta + A(K_1)_{\beta\beta}\right]U_\alpha + \cdots \\ 2\left[A_{\alpha\beta}K_1 + A_\alpha(K_1)_\beta + A_\beta(K_1)_\alpha + A(K_1)_{\alpha\beta}\right]U_\beta + \cdots \\ \begin{bmatrix} A_{\alpha\beta\beta}K_1 + A_{\beta\beta}(K_1)_\alpha + 2A_{\alpha\beta}(K_1)_\beta + \cdots \\ 2A_\beta(K_1)_{\alpha\beta} + A_\alpha(K_1)_{\beta\beta} + A(K_1)_{\alpha\beta\beta} \end{bmatrix} U + W_{\alpha\alpha\beta\beta} \end{Bmatrix}, \tag{D12}$$

$$(\vartheta_2)_{\alpha\alpha\beta} = \frac{1}{B}\begin{Bmatrix} -B_\beta(\vartheta_2)_{\alpha\alpha} - 2B_\alpha(\vartheta_2)_{\alpha\beta} - 2B_{\alpha\beta}(\vartheta_2)_\alpha - B_{\alpha\alpha}(\vartheta_2)_\beta - B_{\alpha\alpha\beta}\vartheta_2 + \cdots \\ BK_2V_{\alpha\alpha\beta} + \left[B_\beta K_2 + B(K_2)_\beta\right]V_{\alpha\alpha} + 2[B_\alpha K_2 + B(K_2)_\alpha]V_{\alpha\beta} + \cdots \\ 2\left[B_{\alpha\beta}K_2 + B_\alpha(K_2)_\beta + B_\beta(K_2)_\alpha + B(K_2)_{\alpha\beta}\right]V_\alpha + \cdots \\ [B_{\alpha\alpha}K_2 + 2B_\alpha(K_2)_\alpha + B(K_2)_{\alpha\alpha}]V_\beta + \cdots \\ \begin{bmatrix} B_{\alpha\alpha\beta}K_2 + B_{\alpha\alpha}(K_2)_\beta + 2B_{\alpha\beta}(K_2)_\alpha + \cdots \\ 2B_\alpha(K_2)_{\alpha\beta} + B_\beta(K_2)_{\alpha\alpha} + B(K_2)_{\alpha\alpha\beta} \end{bmatrix} V - W_{\alpha\alpha\beta\beta} \end{Bmatrix}, \tag{D13}$$

$$(\vartheta_2)_{\beta\beta\beta} = \frac{1}{B}\begin{Bmatrix} -3B_\beta(\vartheta_2)_{\beta\beta} - 3B_{\beta\beta}(\vartheta_2)_\beta - B_{\beta\beta\beta}\vartheta_2 + \cdots \\ BK_2V_{\beta\beta\beta} + 3\left[B_\beta K_2 + B(K_2)_\beta\right]V_{\beta\beta} + \cdots \\ 3\left[B_{\beta\beta}K_2 + 2B_\beta(K_2)_\beta + B(K_2)_{\beta\beta}\right]V_\beta + \cdots \\ [B_{\beta\beta\beta}K_2 + 3B_{\beta\beta}(K_2)_\beta + 3B_\beta(K_2)_{\beta\beta} + B(K_2)_{\beta\beta\beta}]V - W_{\beta\beta\beta\beta} \end{Bmatrix}. \tag{D14}$$

APPENDIX E

Some equations in Section (2) and in Appendices B-D contain spatial derivatives up to the 3rd order of the Lamé parameters. By performing the derivatives of Eqs. (4,5), one obtains

$$A_\alpha = \frac{1}{A}(x_\alpha x_{\alpha\alpha} + y_\alpha y_{\alpha\alpha} + z_\alpha z_{\alpha\alpha}) \tag{E1}$$

$$A_\beta = \frac{1}{A}\left(x_\alpha x_{\alpha\beta} + y_\alpha y_{\alpha\beta} + z_\alpha z_{\alpha\beta}\right) \tag{E2}$$

$$A_{\alpha\alpha} = \frac{1}{A}\begin{pmatrix} -A_\alpha^2 + x_{\alpha\alpha}^2 + y_{\alpha\alpha}^2 + z_{\alpha\alpha}^2 + \cdots \\ x_\alpha x_{\alpha\alpha\alpha} + y_\alpha y_{\alpha\alpha\alpha} + z_\alpha z_{\alpha\alpha\alpha} \end{pmatrix} \tag{E3}$$

$$A_{\alpha\beta} = \frac{1}{A}\begin{pmatrix} -A_\alpha A_\beta + x_{\alpha\alpha}x_{\alpha\beta} + y_{\alpha\alpha}y_{\alpha\beta} + z_{\alpha\alpha}z_{\alpha\beta} + \cdots \\ x_\alpha x_{\alpha\alpha\beta} + y_\alpha y_{\alpha\alpha\beta} + z_\alpha z_{\alpha\alpha\beta} \end{pmatrix} \tag{E4}$$

$$A_{\beta\beta} = \frac{1}{A}\begin{pmatrix} -A_\beta^2 + x_{\beta\beta}^2 + y_{\beta\beta}^2 + z_{\beta\beta}^2 + \cdots \\ x_\alpha x_{\alpha\beta\beta} + y_\alpha y_{\alpha\beta\beta} + z_\alpha z_{\alpha\beta\beta} \end{pmatrix} \tag{E5}$$

Journal of Vibration and Acoustics. Received December 07, 2017;
Accepted manuscript posted July 20, 2018. doi:10.1115/1.4040926

$$A_{\alpha\alpha\alpha} = \frac{1}{A}\begin{pmatrix} -3A_{\alpha\alpha}A_{\alpha} + 3x_{\alpha\alpha}x_{\alpha\alpha\alpha} + 3y_{\alpha\alpha}y_{\alpha\alpha\alpha} + 3z_{\alpha\alpha}z_{\alpha\alpha\alpha} + \cdots \\ x_{\alpha}x_{\alpha\alpha\alpha\alpha} + y_{\alpha}y_{\alpha\alpha\alpha\alpha} + z_{\alpha}z_{\alpha\alpha\alpha\alpha} \end{pmatrix} \tag{E6}$$

$$A_{\alpha\alpha\beta} = \frac{1}{A}\begin{pmatrix} -2A_{\alpha}A_{\alpha\beta} - A_{\beta}A_{\alpha\alpha} + \cdots \\ 2x_{\alpha\alpha}x_{\alpha\alpha\beta} + 2y_{\alpha\alpha}y_{\alpha\alpha\beta} + 3z_{\alpha\alpha}z_{\alpha\alpha\beta} + \cdots \\ x_{\alpha\beta}x_{\alpha\alpha\alpha} + y_{\alpha\beta}y_{\alpha\alpha\alpha} + z_{\alpha\beta}z_{\alpha\alpha\alpha} + \cdots \\ x_{\alpha}x_{\alpha\alpha\alpha\beta} + y_{\alpha}y_{\alpha\alpha\alpha\beta} + z_{\alpha}z_{\alpha\alpha\alpha\beta} \end{pmatrix} \tag{E7}$$

$$A_{\alpha\beta\beta} = \frac{1}{A}\begin{pmatrix} -2A_{\beta}A_{\alpha\beta} - A_{\alpha}A_{\beta\beta} + \cdots \\ 2x_{\alpha\beta}x_{\alpha\alpha\beta} + 2y_{\alpha\beta}y_{\alpha\alpha\beta} + 3z_{\alpha\beta}z_{\alpha\alpha\beta} + \cdots \\ x_{\alpha\alpha}x_{\alpha\beta\beta} + y_{\alpha\alpha}y_{\alpha\beta\beta} + z_{\alpha\alpha}z_{\alpha\beta\beta} + \cdots \\ x_{\alpha}x_{\alpha\alpha\beta\beta} + y_{\alpha}y_{\alpha\alpha\beta\beta} + z_{\alpha}z_{\alpha\alpha\beta\beta} \end{pmatrix} \tag{E8}$$

$$A_{\beta\beta\beta} = \frac{1}{A}\begin{pmatrix} -3A_{\beta\beta}A_{\beta} + 3x_{\alpha\beta}x_{\alpha\beta\beta} + 3y_{\alpha\beta}y_{\alpha\beta\beta} + 3z_{\alpha\beta}z_{\alpha\beta\beta} + \cdots \\ x_{\alpha}x_{\alpha\beta\beta\beta} + y_{\alpha}y_{\alpha\beta\beta\beta} + z_{\alpha}z_{\alpha\beta\beta\beta} \end{pmatrix} \tag{E9}$$

$$B_{\alpha} = \frac{1}{B}\left(x_{\beta}x_{\alpha\beta} + y_{\beta}y_{\alpha\beta} + z_{\beta}z_{\alpha\beta}\right) \tag{E10}$$

$$B_{\beta} = \frac{1}{B}\left(x_{\beta}x_{\beta\beta} + y_{\beta}y_{\beta\beta} + z_{\beta}z_{\beta\beta}\right) \tag{E11}$$

$$B_{\alpha\alpha} = \frac{1}{B}\begin{pmatrix} -B_{\alpha}^2 + x_{\alpha\beta}^2 + y_{\alpha\beta}^2 + z_{\alpha\beta}^2 + \cdots \\ x_{\beta}x_{\alpha\alpha\beta} + y_{\beta}y_{\alpha\alpha\beta} + z_{\beta}z_{\alpha\alpha\beta} \end{pmatrix} \tag{E12}$$

$$B_{\alpha\beta} = \frac{1}{B}\begin{pmatrix} -B_{\alpha}B_{\beta} + x_{\beta\beta}x_{\alpha\beta} + y_{\beta\beta}y_{\alpha\beta} + z_{\beta\beta}z_{\alpha\beta} + \cdots \\ x_{\beta}x_{\alpha\beta\beta} + y_{\beta}y_{\alpha\beta\beta} + z_{\beta}z_{\alpha\beta\beta} \end{pmatrix} \tag{E13}$$

$$B_{\beta\beta} = \frac{1}{B}\begin{pmatrix} -B_{\beta}^2 + x_{\beta\beta}^2 + y_{\beta\beta}^2 + z_{\beta\beta}^2 + \cdots \\ x_{\beta}x_{\beta\beta\beta} + y_{\beta}y_{\beta\beta\beta} + z_{\beta}z_{\beta\beta\beta} \end{pmatrix} \tag{E14}$$

$$B_{\alpha\alpha\alpha} = \frac{1}{B}\begin{pmatrix} -3B_{\alpha\alpha}B_{\alpha} + 3x_{\alpha\beta}x_{\alpha\alpha\beta} + 3y_{\alpha\beta}y_{\alpha\alpha\beta} + 3z_{\alpha\beta}z_{\alpha\alpha\beta} + \cdots \\ x_{\beta}x_{\alpha\alpha\alpha\beta} + y_{\beta}y_{\alpha\alpha\alpha\beta} + z_{\beta}z_{\alpha\alpha\alpha\beta} \end{pmatrix} \tag{E15}$$

$$B_{\alpha\alpha\beta} = \frac{1}{B}\begin{pmatrix} -2B_{\alpha}B_{\alpha\beta} - B_{\beta}B_{\alpha\alpha} + \cdots \\ 2x_{\alpha\beta}x_{\alpha\beta\beta} + 2y_{\alpha\beta}y_{\alpha\beta\beta} + 3z_{\alpha\beta}z_{\alpha\beta\beta} + \cdots \\ x_{\beta\beta}x_{\alpha\alpha\beta} + y_{\beta\beta}y_{\alpha\alpha\beta} + z_{\beta\beta}z_{\alpha\alpha\beta} + \cdots \\ x_{\beta}x_{\alpha\alpha\beta\beta} + y_{\beta}y_{\alpha\alpha\beta\beta} + z_{\beta}z_{\alpha\alpha\beta\beta} \end{pmatrix} \tag{E16}$$

$$B_{\alpha\beta\beta} = \frac{1}{B}\begin{pmatrix} -2B_{\beta}B_{\alpha\beta} - B_{\alpha}B_{\beta\beta} + \cdots \\ 2x_{\beta\beta}x_{\alpha\beta\beta} + 2y_{\beta\beta}y_{\alpha\beta\beta} + 3z_{\beta\beta}z_{\alpha\beta\beta} + \cdots \\ x_{\alpha\beta}x_{\beta\beta\beta} + y_{\alpha\beta}y_{\beta\beta\beta} + z_{\alpha\beta}z_{\beta\beta\beta} + \cdots \\ x_{\beta}x_{\alpha\beta\beta\beta} + y_{\beta}y_{\alpha\beta\beta\beta} + z_{\beta}z_{\alpha\beta\beta\beta} \end{pmatrix} \tag{E17}$$

$$B_{\beta\beta\beta} = \frac{1}{B}\begin{pmatrix} -3B_{\beta\beta}B_{\beta} + 3x_{\beta\beta}x_{\beta\beta\beta} + 3y_{\beta\beta}y_{\beta\beta\beta} + 3z_{\beta\beta}z_{\beta\beta\beta} + \cdots \\ x_{\beta}x_{\beta\beta\beta\beta} + y_{\beta}y_{\beta\beta\beta\beta} + z_{\beta}z_{\beta\beta\beta\beta} \end{pmatrix} \tag{E18}$$

APPENDIX F

The format of Eq. (F1) is identical to the format of Eqs.(31-32) and Eqs. (53-54). When the spatial derivatives of the Eqs.(31-32) are carried out, the symbols Φ and Φ^*

Journal of Vibration and Acoustics. Received December 07, 2017;
Accepted manuscript posted July 20, 2018. doi:10.1115/1.4040926

are substituted by the Lamé parameters from the middle surface (A or B) and the outer surface (A^{γ} or B^{γ}, for $\gamma = h/2$), respectively. When Eqs. (53-54) are analyzed, Φ and Φ^* are respectively substituted by $\widetilde{U}$ or $\widetilde{V}$ and U^* or V^*.

$$\Phi = \Pi_d \Phi^*, \tag{F1}$$

$$(\Phi)_\alpha = \Pi_d (\Phi^*)_\alpha + (\Pi_d)_\alpha \Phi^*, \tag{F2}$$

$$(\Phi)_\beta = \Pi_d (\Phi^*)_\beta + (\Pi_d)_\beta \Phi^*, \tag{F3}$$

$$(\Phi)_{\alpha\alpha} = \Pi_d (\Phi^*)_{\alpha\alpha} + 2(\Pi_d)_\alpha (\Phi^*)_\alpha + (\Pi_d)_{\alpha\alpha} \Phi^*, \tag{F4}$$

$$(\Phi)_{\alpha\beta} = (\Pi_d)_\beta (\Phi^*)_\alpha + \Pi_d (\Phi^*)_{\alpha\beta} + (\Pi_d)_{\alpha\beta} \Phi^* + (\Pi_d)_{\alpha\beta} \Phi^* + (\Pi_d)_\alpha (\Phi^*)_\beta, \tag{F5}$$

$$(\Phi)_{\beta\beta} = \Pi_d (\Phi^*)_{\beta\beta} + 2(\Pi_d)_\beta (\Phi^*)_\beta + (\Pi_d)_{\beta\beta} \Phi^*, \tag{F6}$$

$$(\Phi)_{\alpha\alpha\alpha} = \Pi_d (\Phi^*)_{\alpha\alpha\alpha} + 3(\Pi_d)_\alpha (\Phi^*)_{\alpha\alpha} + 3(\Pi_d)_{\alpha\alpha} (\Phi^*)_\alpha + (\Pi_d)_{\alpha\alpha\alpha} \Phi^*, \tag{F7}$$

$$\begin{gathered}(\Phi)_{\alpha\alpha\beta} = \Pi_d (\Phi^*)_{\alpha\alpha\beta} + 2(\Pi_d)_\alpha (\Phi^*)_{\alpha\beta} + 2(\Pi_d)_{\alpha\beta} (\Phi^*)_\alpha + \cdots \\ (\Pi_d)_{\alpha\alpha} (\Phi^*)_\beta + (\Pi_d)_{\alpha\alpha\beta} \Phi^* + (\Pi_d)_\beta (\Phi^*)_{\alpha\alpha},\end{gathered} \tag{F8}$$

$$\begin{gathered}(\Phi)_{\alpha\beta\beta} = \Pi_d (\Phi^*)_{\alpha\beta\beta} + 2(\Pi_d)_\beta (\Phi^*)_{\alpha\beta} + 2(\Pi_d)_{\alpha\beta} (\Phi^*)_\beta + \cdots \\ (\Pi_d)_{\beta\beta} (\Phi^*)_\alpha + (\Pi_d)_{\alpha\beta\beta} \Phi^* + (\Pi_d)_\alpha (\Phi^*)_{\beta\beta},\end{gathered} \tag{F9}$$

$$(\Phi)_{\beta\beta\beta} = \Pi_d (\Phi^*)_{\beta\beta\beta} + 3(\Pi_d)_\beta (\Phi^*)_{\beta\beta} + 3(\Pi_d)_{\beta\beta} (\Phi^*)_\beta + (\Pi_d)_{\beta\beta\beta} \Phi^*. \tag{F10}$$

Derivatives up to the 3rd order of the curvature coefficients are present in Eqs. (F1 - F10). They can be directly obtained from Eq. (33), yielding

$$(\Pi_d)_\alpha = \gamma (\Pi_d)^2 (K_d)_\alpha, \tag{F11}$$

$$(\Pi_d)_\beta = \gamma (\Pi_d)^2 (K_d)_\beta, \tag{F12}$$

$$(\Pi_d)_{\alpha\alpha} = \gamma (\Pi_d)^2 (K_d)_{\alpha\alpha} + 2\gamma \Pi_n (K_d)_\alpha (\Pi_d)_\alpha, \tag{F13}$$

Journal of Vibration and Acoustics. Received December 07, 2017;
Accepted manuscript posted July 20, 2018. doi:10.1115/1.4040926

$$(\Pi_d)_{\alpha\beta} = \gamma(\Pi_d)^2(K_d)_{\alpha\beta} + 2(1-\gamma K_d)(\Pi_d)_\alpha(\Pi_d)_\beta, \tag{F14}$$

$$(\Pi_d)_{\beta\beta} = \gamma(\Pi_d)^2(K_d)_{\beta\beta} + 2\gamma\Pi_d(K_d)_\beta(\Pi_d)_\beta, \tag{F15}$$

$$(\Pi_d)_{\alpha\alpha\alpha} = \gamma(\Pi_d)^2(K_d)_{\alpha\alpha\alpha} + 4\gamma\Pi_d(\Pi_d)_\alpha(K_d)_{\alpha\alpha} + 2\gamma(K_d)_\alpha[(\Pi_d)_\alpha^2 + \Pi_d(\Pi_d)_{\alpha\alpha}], \tag{F16}$$

$$\begin{gathered}(\Pi_d)_{\alpha\alpha\beta} = \gamma(\Pi_d)^2(K_d)_{\alpha\alpha\beta} + 2\gamma\Pi_d(\Pi_d)_\beta(K_d)_{\alpha\alpha} + 2\gamma\Pi_d(\Pi_d)_\alpha(K_d)_{\alpha\beta} + \cdots \\ 2\gamma(K_d)_\alpha\big[(\Pi_d)_\alpha(\Pi_d)_\beta + \Pi_d(\Pi_d)_{\alpha\beta}\big],\end{gathered} \tag{F17}$$

$$\begin{gathered}(\Pi_d)_{\alpha\beta\beta} = \gamma(\Pi_d)^2(K_d)_{\alpha\beta\beta} + 2\gamma\Pi_d(\Pi_d)_\alpha(K_d)_{\beta\beta} + 2\gamma\Pi_d(\Pi_d)_\beta(K_d)_{\alpha\beta} + \cdots \\ 2\gamma(K_d)_\beta\big[(\Pi_d)_\alpha(\Pi_d)_\beta + \Pi_d(\Pi_d)_{\alpha\beta}\big],\end{gathered} \tag{F18}$$

$$(\Pi_d)_{\beta\beta\beta} = \gamma(\Pi_d)^2(K_d)_{\beta\beta\beta} + 4\gamma\Pi_d(\Pi_d)_\beta(K_d)_{\beta\beta} + 2\gamma(K_d)_\beta\big[(\Pi_d)_\beta^2 + \Pi_d(\Pi_d)_{\beta\beta}\big]. \tag{F19}$$

APPENDIX G

All of the coefficients of the PDs, which are defined with respect to the standard Cartesian triad of unit vectors (Eqs.(40-42)), are a function of the spatial derivative of the surface's "height" (z coordinate) with respect to x and y. The expressions are [18]

$$q_1 = \frac{1}{\sqrt{1+z_x^2}}, \tag{G1}$$

$$s_1 = \frac{z_x}{\sqrt{1+z_x^2}}, \tag{G2}$$

$$r_2 = \frac{1}{\sqrt{1+z_y^2}}, \tag{G3}$$

$$s_2 = \frac{z_y}{\sqrt{1+z_y^2}}, \tag{G4}$$

$$q_3 = -\frac{z_x}{\sqrt{1+z_x^2+z_y^2}}, \tag{G5}$$

$$r_3 = -\frac{z_y}{\sqrt{1+z_x^2+z_y^2}}, \tag{G6}$$

$$s_3 = \frac{1}{\sqrt{1+z_x^2+z_y^2}}. \tag{G7}$$

Journal of Vibration and Acoustics. Received December 07, 2017;
Accepted manuscript posted July 20, 2018. doi:10.1115/1.4040926

Before calculating the TCs $(\rho_1, \psi_1, \rho_2, \psi_2)$ present in Eq.(43), the tangent PCDs are defined with respect to the Cartesian basis vectors $\mathbf{i}$, $\mathbf{j}$ and $\mathbf{k}$ as follows:

$$\mathbf{e_1} = f_1\mathbf{i} + g_1\mathbf{j} + h_1\mathbf{k}, \tag{G8}$$

$$\mathbf{e_2} = f_2\mathbf{i} + g_2\mathbf{j} + h_2\mathbf{k}. \tag{G9}$$

The TCs can now be obtained from the tangent PCDs (Eqs.(G8-G9)) and PDs (Eqs.(40-42)) in the standard basis. By rearranging equations, the TCs can be assessed by

$$\rho_d = \frac{1}{q_1r_2s_3 - q_1s_2r_3 - s_1r_2q_3}[(r_2s_3 - s_2r_3)f_d + (s_2q_3)g_d + (-r_2q_3)h_d], \text{for } d = \{1,2\}, \tag{G10}$$

$$\psi_d = \frac{1}{q_1r_2s_3 - q_1s_2r_3 - s_1r_2q_3}[(s_1r_3)f_d + (q_1s_3 - s_1q_3)g_d + (-q_1r_3)h_d], \text{for } d = \{1,2\}. \tag{G11}$$

APPENDIX H

By applying the chain rule on Eq.(49), higher-order spatial derivatives with respect to the $\alpha\beta$-space can be assessed. The equations presented below are spatial derivatives ranging from the 2nd up to the 4th order:

$$\Phi_{\alpha\alpha} = \Phi_{xx}(x_\alpha^2) + \Phi_{xy}(x_\alpha y_\alpha) + \Phi_{yy}(y_\alpha^2) + \Phi_x x_{\alpha\alpha} + \Phi_y y_{\alpha\alpha} \tag{H1}$$

$$\Phi_{\alpha\beta} = \Phi_{xx}(x_\alpha x_\beta) + \Phi_{xy}\left(x_\alpha y_\beta + x_\beta y_\alpha\right) + \Phi_{yy}(y_\alpha y_\beta) + \Phi_x x_{\alpha\beta} + \Phi_y y_{\alpha\beta} \tag{H2}$$

$$\Phi_{\beta\beta} = \Phi_{xx}(x_\beta^2) + \Phi_{xy}\left(x_\beta y_\beta\right) + \Phi_{yy}(y_\beta^2) + \Phi_x x_{\beta\beta} + \Phi_y y_{\beta\beta} \tag{H3}$$

$$\begin{aligned}\Phi_{\alpha\alpha\alpha} = {} & \Phi_{xxx}(x_\alpha^3) + \Phi_{xxy}(3x_\alpha^2 y_\alpha) + \Phi_{xyy}(x_\alpha y_\alpha^2) + \Phi_{yyy}(y_\alpha^3) + \cdots \\ & \Phi_{xx}(3x_{\alpha\alpha}x_\alpha) + \Phi_{xy}(3x_{\alpha\alpha}y_\alpha + 3x_\alpha y_{\alpha\alpha}) + \Phi_{yy}(3y_{\alpha\alpha}y_\alpha) + \cdots \\ & \Phi_x x_{\alpha\alpha\alpha} + \Phi_y y_{\alpha\alpha\alpha}\end{aligned} \tag{H4}$$

$$\begin{aligned}\Phi_{\alpha\alpha\beta} = {} & \Phi_{xxx}(x_\alpha^2 y_\beta) + \Phi_{xxy}\left(2x_\alpha x_\beta y_\alpha + x_\alpha^2 y_\beta\right) + \cdots \\ & \Phi_{xyy}(x_\beta y_\alpha^2 + 2x_\alpha y_\alpha y_\beta) + \Phi_{yyy}(y_\alpha^2 y_\beta) + \cdots \\ & \Phi_{xx}\left(x_{\alpha\alpha}x_\beta + 2x_\alpha x_{\alpha\beta}\right) + \cdots \\ & \Phi_{xy}\left(x_{\alpha\alpha}y_\beta + 2x_{\alpha\beta}y_\alpha + 2x_\alpha y_{\alpha\beta} + x_\beta y_{\alpha\alpha}\right) + \cdots\end{aligned} \tag{H5}$$

Journal of Vibration and Acoustics. Received December 07, 2017;
Accepted manuscript posted July 20, 2018. doi:10.1115/1.4040926

$$\Phi_{yy}\left(y_{\alpha\alpha}y_{\beta}+2y_{\alpha}y_{\alpha\beta}\right)+\Phi_{x}x_{\alpha\alpha\beta}+\Phi_{y}y_{\alpha\alpha\beta}$$

$$\begin{aligned}\Phi_{\alpha\beta\beta}=&\ \Phi_{xxx}\left(x_{\alpha}x_{\beta}^{2}\right)+\Phi_{xxy}\left(2x_{\alpha}x_{\beta}y_{\beta}+x_{\beta}^{2}y_{\alpha}\right)+\cdots\\&\Phi_{xyy}(x_{\alpha}y_{\beta}^{2}+2x_{\beta}y_{\alpha}y_{\beta})+\Phi_{yyy}(y_{\alpha}y_{\beta}^{2})+\cdots\\&\Phi_{xx}\left(x_{\alpha}x_{\beta\beta}+2x_{\beta}x_{\alpha\beta}\right)+\cdots\\&\Phi_{xy}\left(x_{\beta\beta}y_{\alpha}+2x_{\alpha\beta}y_{\beta}+2x_{\beta}y_{\alpha\beta}+x_{\alpha}y_{\beta\beta}\right)+\cdots\\&\Phi_{yy}\left(y_{\beta\beta}y_{\alpha}+2y_{\beta}y_{\alpha\beta}\right)+\Phi_{x}x_{\alpha\beta\beta}+\Phi_{y}y_{\alpha\beta\beta}\end{aligned}\tag{H6}$$

$$\begin{aligned}\Phi_{\beta\beta\beta}=&\ \Phi_{xxx}(x_{\beta}^{3})+\Phi_{xxy}\left(3x_{\beta}^{2}y_{\beta}\right)+\Phi_{xyy}(x_{\beta}y_{\beta}^{2})+\Phi_{yyy}(y_{\beta}^{3})+\cdots\\&\Phi_{xx}\left(3x_{\beta\beta}x_{\beta}\right)+\Phi_{xy}\left(3x_{\beta\beta}y_{\beta}+3x_{\beta}y_{\beta\beta}\right)+\Phi_{yy}\left(3y_{\beta\beta}y_{\beta}\right)+\cdots\\&\Phi_{x}x_{\beta\beta\beta}+\Phi_{y}y_{\beta\beta\beta}\end{aligned}\tag{H7}$$

$$\begin{aligned}\Phi_{\alpha\alpha\alpha\alpha}=&\ \Phi_{xxxx}(x_{\alpha}^{4})+\Phi_{xxxy}(4x_{\alpha}^{3}y_{\alpha})+\Phi_{xxyy}(6x_{\alpha}^{2}y_{\alpha}^{2})+\Phi_{xyyy}(4x_{\alpha}y_{\alpha}^{3})+\Phi_{yyyy}(y_{\alpha}^{4})+\cdots\\&\Phi_{xxx}(6x_{\alpha}^{2}x_{\alpha\alpha})+\Phi_{xxy}(6x_{\alpha}^{2}y_{\alpha\alpha}+12x_{\alpha\alpha}x_{\alpha}y_{\alpha})+\cdots\\&\Phi_{xyy}(6y_{\alpha}^{2}x_{\alpha\alpha}+12y_{\alpha\alpha}x_{\alpha}y_{\alpha})+\Phi_{yyy}(6y_{\alpha}^{2}y_{\alpha\alpha})+\cdots\\&\Phi_{xx}(4x_{\alpha\alpha\alpha}x_{\alpha}+3x_{\alpha\alpha}^{2})+\Phi_{xy}(4x_{\alpha\alpha\alpha}y_{\alpha}+6x_{\alpha\alpha}y_{\alpha\alpha}+4y_{\alpha\alpha\alpha}x_{\alpha})+\cdots\\&\Phi_{yy}(4y_{\alpha\alpha\alpha}y_{\alpha}+3y_{\alpha\alpha}^{2})+\Phi_{x}x_{\alpha\alpha\alpha\alpha}+\Phi_{y}y_{\alpha\alpha\alpha\alpha}\end{aligned}\tag{H8}$$

$$\begin{aligned}\Phi_{\alpha\alpha\alpha\beta}=&\ \Phi_{xxxx}\left(x_{\alpha}^{3}x_{\beta}\right)+\Phi_{xxxy}\left(x_{\alpha}^{3}y_{\beta}+3x_{\alpha}^{2}x_{\beta}y_{\alpha}\right)+\cdots\\&\Phi_{xxyy}\left(3x_{\alpha}^{2}y_{\alpha}y_{\beta}+3x_{\alpha}x_{\beta}y_{\alpha}^{2}\right)+\cdots\\&\Phi_{xyyy}\left(y_{\alpha}^{3}x_{\beta}+3x_{\alpha}y_{\alpha}^{2}y_{\beta}\right)+\Phi_{yyyy}\left(y_{\alpha}^{3}y_{\beta}\right)+\cdots\\&\Phi_{xxx}\left(3x_{\alpha\alpha}x_{\alpha}x_{\beta}+3x_{\alpha\beta}x_{\alpha}^{2}\right)+\cdots\\&\Phi_{xxy}\left(3x_{\alpha\alpha}x_{\beta}y_{\alpha}+3x_{\alpha\alpha}x_{\alpha}y_{\beta}+6x_{\alpha\beta}x_{\alpha}y_{\alpha}+3y_{\alpha\beta}x_{\alpha}^{2}+3x_{\alpha}x_{\beta}y_{\alpha\alpha}\right)+\cdots\\&\Phi_{xyy}\left(3y_{\alpha\alpha}x_{\beta}y_{\alpha}+3y_{\alpha\alpha}x_{\alpha}y_{\beta}+6y_{\alpha\beta}x_{\alpha}y_{\alpha}+3x_{\alpha\beta}y_{\alpha}^{2}+3x_{\alpha\alpha}y_{\alpha}y_{\beta}\right)+\cdots\\&\Phi_{yyy}\left(3y_{\alpha\alpha}y_{\alpha}y_{\beta}+3y_{\alpha\beta}y_{\alpha}^{2}\right)+\cdots\\&\Phi_{xx}\left(x_{\alpha\alpha\alpha}x_{\beta}+3x_{\alpha\alpha\beta}x_{\alpha}+3x_{\alpha\alpha}x_{\alpha\beta}\right)+\cdots\\&\Phi_{xy}\left(x_{\alpha\alpha\alpha}y_{\beta}+3x_{\alpha\alpha\beta}y_{\alpha}+3x_{\alpha\beta}y_{\alpha\alpha}+3x_{\alpha\alpha}y_{\alpha\beta}+3x_{\alpha}y_{\alpha\alpha\beta}+x_{\beta}y_{\alpha\alpha\alpha}\right)+\cdots\\&\Phi_{yy}\left(y_{\alpha\alpha\alpha}y_{\beta}+3y_{\alpha\alpha\beta}y_{\alpha}+3y_{\alpha\alpha}y_{\alpha\beta}\right)+\Phi_{x}x_{\alpha\alpha\alpha\beta}+\Phi_{y}y_{\alpha\alpha\alpha\beta}\end{aligned}\tag{H9}$$

$$\begin{aligned}\Phi_{\alpha\alpha\beta\beta}=&\ \Phi_{xxxx}(x_{\alpha}^{2}x_{\beta}^{2})+\Phi_{xxxy}\left(2x_{\alpha}^{2}x_{\beta}y_{\beta}+2x_{\alpha}x_{\beta}^{2}y_{\alpha}\right)+\cdots\\&\Phi_{xxyy}\left(x_{\alpha}^{2}y_{\beta}^{2}+4x_{\alpha}x_{\beta}y_{\alpha}y_{\beta}+x_{\beta}^{2}y_{\alpha}^{2}\right)+\cdots\\&\Phi_{xyyy}\left(2x_{\beta}y_{\alpha}^{2}y_{\beta}+2x_{\alpha}y_{\alpha}y_{\beta}^{2}\right)+\Phi_{yyyy}(y_{\alpha}^{2}y_{\beta}^{2})+\cdots\\&\Phi_{xxx}\left(4x_{\alpha\beta}x_{\alpha}y_{\beta}+x_{\alpha\alpha}x_{\beta}^{2}+x_{\beta\beta}x_{\alpha}^{2}\right)+\cdots\end{aligned}\tag{H10}$$

Journal of Vibration and Acoustics. Received December 07, 2017;
Accepted manuscript posted July 20, 2018. doi:10.1115/1.4040926

$$\Phi_{xxy}\begin{pmatrix}2x_{\alpha\alpha}x_\beta y_\beta + 4x_{\alpha\beta}x_\alpha y_\beta + 4x_{\alpha\beta}x_\beta y_\alpha + \cdots \\ 2x_{\beta\beta}x_\alpha y_\alpha + 4y_{\alpha\beta}x_\alpha x_\beta + x_\beta^2 y_{\alpha\alpha} + x_\alpha^2 y_{\beta\beta}\end{pmatrix} + \cdots$$

$$\Phi_{xyy}\begin{pmatrix}2y_{\alpha\alpha}x_\beta y_\beta + 4y_{\alpha\beta}x_\alpha y_\beta + 4y_{\alpha\beta}x_\beta y_\alpha + \cdots \\ 2y_{\beta\beta}x_\alpha y_\alpha + 4x_{\alpha\beta}y_\alpha y_\beta + y_\beta^2 x_{\alpha\alpha} + y_\alpha^2 x_{\beta\beta}\end{pmatrix} + \cdots$$

$$\Phi_{yyy}\left(4y_{\alpha\beta}y_\alpha y_\beta + y_{\alpha\alpha}y_\beta^2 + y_{\beta\beta}y_\alpha^2\right) + \cdots$$

$$\Phi_{xx}\left(2x_{\alpha\alpha\beta}x_\beta + 2x_{\alpha\beta\beta}x_\alpha + x_{\alpha\alpha}x_{\beta\beta} + 2x_{\alpha\beta}^2\right) + \cdots$$

$$\Phi_{xy}\begin{pmatrix}2x_{\alpha\alpha\beta}y_\beta + 2x_{\alpha\beta\beta}y_\alpha + x_{\alpha\alpha}y_{\beta\beta} + \cdots \\ 4x_{\alpha\beta}y_{\alpha\beta} + x_{\beta\beta}y_{\alpha\alpha} + 2x_\alpha y_{\alpha\beta\beta} + 2x_\beta y_{\alpha\alpha\beta}\end{pmatrix} + \cdots$$

$$\Phi_{yy}\left(2y_{\alpha\alpha\beta}y_\beta + 2y_{\alpha\beta\beta}y_\alpha + y_{\alpha\alpha}y_{\beta\beta} + 2y_{\alpha\beta}^2\right) + \Phi_x x_{\alpha\alpha\beta\beta} + \Phi_y y_{\alpha\alpha\beta\beta}$$

$$\Phi_{\alpha\beta\beta\beta} = \Phi_{xxxx}\left(x_\beta^3 x_\alpha\right) + \Phi_{xxxy}\left(x_\beta^3 y_\alpha + 3x_\beta^2 x_\alpha y_\beta\right) + \cdots$$

$$\Phi_{xxyy}\left(3x_\beta^2 y_\beta y_\alpha + 3x_\beta x_\alpha y_\beta^2\right) + \cdots$$

$$\Phi_{xyyy}\left(y_\beta^3 x_\alpha + 3x_\beta y_\beta^2 y_\alpha\right) + \Phi_{yyyy}\left(y_\beta^3 y_\alpha\right) + \cdots$$

$$\Phi_{xxx}\left(3x_{\beta\beta}x_\alpha x_\beta + 3x_{\alpha\beta}x_\beta^2\right) + \cdots$$

$$\Phi_{xxy}\left(3x_{\beta\beta}x_\alpha y_\beta + 3x_{\beta\beta}x_\beta y_\alpha + 6x_{\alpha\beta}x_\beta y_\beta + 3y_{\alpha\beta}x_\beta^2 + 3x_\alpha x_\beta y_{\beta\beta}\right) + \cdots \tag{H11}$$

$$\Phi_{xyy}\left(3y_{\beta\beta}x_\alpha y_\beta + 3y_{\beta\beta}x_\beta y_\alpha + 6y_{\alpha\beta}x_\beta y_\beta + 3x_{\alpha\beta}y_\beta^2 + 3x_{\beta\beta}y_\alpha y_\beta\right) + \cdots$$

$$\Phi_{yyy}\left(3y_{\beta\beta}y_\alpha y_\beta + 3y_{\alpha\beta}y_\beta^2\right) + \cdots$$

$$\Phi_{xx}\left(x_{\beta\beta\beta}x_\alpha + 3x_{\alpha\beta\beta}x_\beta + 3x_{\beta\beta}x_{\alpha\beta}\right) + \cdots$$

$$\Phi_{xy}\left(x_{\beta\beta\beta}y_\alpha + 3x_{\alpha\beta\beta}y_\beta + 3x_{\alpha\beta}y_{\beta\beta} + 3x_{\beta\beta}y_{\alpha\beta} + 3x_\beta y_{\alpha\beta\beta} + x_\alpha y_{\beta\beta\beta}\right) + \cdots$$

$$\Phi_{yy}\left(y_{\beta\beta\beta}y_\alpha + 3y_{\alpha\beta\beta}y_\beta + 3y_{\beta\beta}y_{\alpha\beta}\right) + \Phi_x x_{\alpha\beta\beta\beta} + \Phi_y y_{\alpha\beta\beta\beta}$$

$$\Phi_{\beta\beta\beta\beta} = \Phi_{xxxx}\left(x_\beta^4\right) + \Phi_{xxxy}\left(4x_\beta^3 y_\beta\right) + \Phi_{xxyy}\left(6x_\beta^2 y_\beta^2\right) + \Phi_{xyyy}\left(4x_\beta y_\beta^3\right) + \Phi_{yyyy}\left(y_\beta^4\right) + \cdots$$

$$\Phi_{xxx}\left(6x_\beta^2 x_{\beta\beta}\right) + \Phi_{xxy}\left(6x_\beta^2 y_{\beta\beta} + 12x_{\beta\beta}x_\beta y_\beta\right) + \cdots$$

$$\Phi_{xyy}\left(6y_\beta^2 x_{\beta\beta} + 12y_{\beta\beta}x_\beta y_\beta\right) + \Phi_{yyy}\left(6y_\beta^2 y_{\beta\beta}\right) + \cdots \tag{H12}$$

$$\Phi_{xx}\left(4x_{\beta\beta\beta}x_\beta + 3x_{\beta\beta}^2\right) + \Phi_{xy}\left(4x_{\beta\beta\beta}y_\beta + 6x_{\beta\beta}y_{\beta\beta} + 4y_{\beta\beta\beta}x_\beta\right) + \cdots$$

$$\Phi_{yy}\left(4y_{\beta\beta\beta}y_\beta + 3y_{\beta\beta}^2\right) + \Phi_x x_{\beta\beta\beta\beta} + \Phi_y y_{\beta\beta\beta\beta}$$

APPENDIX I

All spatial derivatives of $\widetilde{U}^{h/2}$ and $\widetilde{V}^{h/2}$ can be directly obtained by manipulating the Eqs.(50-51). By considering

$$\tau_1 = \widetilde{U}^{h/2}, \tag{I1}$$

Journal of Vibration and Acoustics. Received December 07, 2017;
Accepted manuscript posted July 20, 2018. doi:10.1115/1.4040926

$$\tau_2 = \tilde{V}^{h/2}, \tag{I2}$$

the following expressions can be derived for the mentioned fields:

$$(\tau_d)_\alpha = \rho_d \hat{U}_\alpha + \psi_d \hat{V}_\alpha + (\rho_d)_\alpha \hat{U} + (\psi_d)_\alpha \hat{V} \tag{I3}$$

$$(\tau_d)_\beta = \rho_d \hat{U}_\beta + \psi_d \hat{V}_\beta + (\rho_d)_\beta \hat{U} + (\psi_d)_\beta \hat{V} \tag{I4}$$

$$(\tau_d)_{\alpha\alpha} = \rho_d \hat{U}_{\alpha\alpha} + 2(\rho_d)_\alpha \hat{U}_\alpha + (\rho_d)_{\alpha\alpha} U + \psi_d \hat{V}_{\alpha\alpha} + 2(\psi_d)_\alpha \hat{V}_\alpha + (\psi_d)_{\alpha\alpha} \hat{V} \tag{I5}$$

$$\begin{gathered}(\tau_d)_{\alpha\beta} = \rho_d \hat{U}_{\alpha\beta} + (\rho_d)_\alpha \hat{U}_\beta + (\rho_d)_\beta \hat{U}_\alpha + (\rho_d)_{\alpha\beta} \hat{U} + \cdots \\ \psi_d \hat{V}_{\alpha\beta} + (\psi_d)_\alpha \hat{V}_\beta + (\psi_d)_\beta \hat{V}_\alpha + (\psi_d)_{\alpha\beta} \hat{V}\end{gathered} \tag{I6}$$

$$(\tau_d)_{\beta\beta} = \rho_d \hat{U}_{\beta\beta} + 2(\rho_d)_\beta \hat{U}_\beta + (\rho_d)_{\beta\beta} U + \psi_d \hat{V}_{\beta\beta} + 2(\psi_d)_\beta \hat{V}_\beta + (\psi_d)_{\beta\beta} \hat{V} \tag{I7}$$

$$\begin{gathered}(\tau_d)_{\alpha\alpha\alpha} = \rho_d \hat{U}_{\alpha\alpha\alpha} + 3(\rho_d)_\alpha \hat{U}_{\alpha\alpha} + 3(\rho_d)_{\alpha\alpha} \hat{U}_\alpha + (\rho_d)_{\alpha\alpha\alpha} \hat{U} + \cdots \\ \psi_d \hat{V}_{\alpha\alpha\alpha} + 3(\psi_d)_\alpha \hat{V}_{\alpha\alpha} + 3(\psi_d)_{\alpha\alpha} \hat{V}_\alpha + (\psi_d)_{\alpha\alpha\alpha} \hat{V}\end{gathered} \tag{I8}$$

$$\begin{gathered}(\tau_d)_{\alpha\alpha\beta} = \rho_d \hat{U}_{\alpha\alpha\beta} + 2(\rho_d)_\alpha \hat{U}_{\alpha\beta} + (\rho_d)_\beta \hat{U}_{\alpha\alpha} + 2(\rho_d)_{\alpha\beta} \hat{U}_\alpha + (\rho_d)_{\alpha\alpha} \hat{U}_\beta + (\rho_d)_{\alpha\alpha\beta} \hat{U} + \cdots \\ \psi_d \hat{V}_{\alpha\alpha\beta} + 2(\psi_d)_\alpha \hat{V}_{\alpha\beta} + (\psi_d)_\beta \hat{V}_{\alpha\alpha} + 2(\psi_d)_{\alpha\beta} \hat{V}_\alpha + (\psi_d)_{\alpha\alpha} \hat{V}_\beta + (\psi_d)_{\alpha\alpha\beta} \hat{V}\end{gathered} \tag{I9}$$

$$\begin{gathered}(\tau_d)_{\alpha\beta\beta} = \rho_d \hat{U}_{\alpha\beta\beta} + 2(\rho_d)_\beta \hat{U}_{\alpha\beta} + (\rho_d)_{\beta\beta} \hat{U}_\alpha + 2(\rho_d)_{\alpha\beta} \hat{U}_\beta + (\rho_d)_\alpha \hat{U}_{\beta\beta} + (\rho_d)_{\alpha\beta\beta} \hat{U} + \cdots \\ \psi_d \hat{V}_{\alpha\beta\beta} + 2(\psi_d)_\beta \hat{V}_{\alpha\beta} + (\psi_d)_\alpha \hat{V}_{\beta\beta} + 2(\psi_d)_{\alpha\beta} \hat{V}_\beta + (\psi_d)_{\beta\beta} \hat{V}_\alpha + (\psi_d)_{\alpha\beta\beta} \hat{V}\end{gathered} \tag{I10}$$

$$\begin{gathered}(\tau_d)_{\beta\beta\beta} = \rho_d \hat{U}_{\beta\beta\beta} + 3(\rho_d)_\beta \hat{U}_{\beta\beta} + 3(\rho_d)_{\beta\beta} \hat{U}_\beta + (\rho_d)_{\beta\beta\beta} \hat{U} + \cdots \\ \psi_d \hat{V}_{\beta\beta\beta} + 3(\psi_d)_\beta \hat{V}_{\beta\beta} + 3(\psi_d)_{\beta\beta} \hat{V}_\beta + (\psi_d)_{\beta\beta\beta} \hat{V}\end{gathered} \tag{I11}$$

APPENDIX J

The spatial derivatives up to the 3rd order of Eqs.(55-56) as a function of γ are shown below:

$$(U^*)_\alpha = (U^\gamma)_\alpha - \frac{\gamma}{A}\left(-\frac{A_\alpha}{A} W_\alpha + W_{\alpha\alpha}\right) \tag{J1}$$

$$(U^*)_\beta = (U^\gamma)_\beta - \frac{\gamma}{A}\left(-\frac{A_\beta}{A} W_\alpha + W_{\alpha\beta}\right) \tag{J2}$$

$$(U^*)_{\alpha\alpha} = (U^\gamma)_{\alpha\alpha} - \frac{\gamma}{A^2}\left[\left(2\frac{A_\alpha^2}{A} - A_{\alpha\alpha}\right) W_\alpha - 2A_\alpha W_{\alpha\alpha} + A W_{\alpha\alpha\alpha}\right] \tag{J3}$$

Journal of Vibration and Acoustics. Received December 07, 2017;
Accepted manuscript posted July 20, 2018. doi:10.1115/1.4040926

$$(U^*)_{\alpha\beta} = (U^\gamma)_{\alpha\beta} - \frac{\gamma}{A^2}\left[\left(2\frac{A_\alpha A_\beta}{A} - A_{\alpha\beta}\right)W_\alpha - A_\beta W_{\alpha\alpha} - A_\alpha W_{\alpha\beta} + AW_{\alpha\alpha\beta}\right] \tag{J4}$$

$$(U^*)_{\beta\beta} = (U^\gamma)_{\beta\beta} - \frac{\gamma}{A^2}\left[\left(2\frac{A_\beta^2}{A} - A_{\beta\beta}\right)W_\alpha - 2A_\beta W_{\alpha\beta} + AW_{\alpha\beta\beta}\right] \tag{J5}$$

$$(U^*)_{\alpha\alpha\alpha} = (U^\gamma)_{\alpha\alpha\alpha} - \frac{\gamma}{A^2}\begin{bmatrix} \left(6\frac{A_\alpha A_{\alpha\alpha}}{A} - 6\frac{A_\alpha^3}{A^2} - A_{\alpha\alpha\alpha}\right)W_\alpha + \cdots \\ \left(6\frac{A_\alpha^2}{A} - 3A_{\alpha\alpha}\right)W_{\alpha\alpha} - 3A_\alpha W_{\alpha\alpha\alpha} + AW_{\alpha\alpha\alpha\alpha} \end{bmatrix} \tag{J6}$$

$$(U^*)_{\alpha\alpha\beta} = (U^\gamma)_{\alpha\alpha\beta} - \frac{\gamma}{A^2}\begin{bmatrix} \left(4\frac{A_\alpha A_{\alpha\beta}}{A} - 6\frac{A_\alpha^2 A_\beta}{A^2} + 2\frac{A_{\alpha\alpha}A_\beta}{A} - A_{\alpha\alpha\beta}\right)W_\alpha + \cdots \\ \left(4\frac{A_\alpha A_\beta}{A} - 2A_{\alpha\beta}\right)W_{\alpha\alpha} + \left(2\frac{A_\alpha^2}{A} - A_{\alpha\alpha}\right)W_{\alpha\beta} - \cdots \\ 2A_\alpha W_{\alpha\alpha\beta} - A_\beta W_{\alpha\alpha\alpha} + AW_{\alpha\alpha\alpha\beta} \end{bmatrix} \tag{J7}$$

$$(U^*)_{\alpha\beta\beta} = (U^\gamma)_{\alpha\beta\beta} - \frac{\gamma}{A^2}\begin{bmatrix} \left(4\frac{A_\beta A_{\alpha\beta}}{A} - 6\frac{A_\alpha A_\beta^2}{A^2} + 2\frac{A_{\beta\beta}A_\alpha}{A} - A_{\alpha\beta\beta}\right)W_\alpha + \cdots \\ \left(2\frac{A_\beta^2}{A} - A_{\beta\beta}\right)W_{\alpha\alpha} + \left(4\frac{A_\alpha A_\beta}{A} - 2A_{\alpha\beta}\right)W_{\alpha\beta} - \cdots \\ 2A_\beta W_{\alpha\alpha\beta} - A_\alpha W_{\alpha\beta\beta} + AW_{\alpha\alpha\beta\beta} \end{bmatrix} \tag{J8}$$

$$(U^*)_{\beta\beta\beta} = (U^\gamma)_{\beta\beta\beta} - \frac{\gamma}{A^2}\begin{bmatrix} \left(6\frac{A_\beta A_{\beta\beta}}{A} - 6\frac{A_\beta^3}{A^2} - A_{\beta\beta\beta}\right)W_\alpha + \cdots \\ \left(6\frac{A_\beta^2}{A} - 3A_{\beta\beta}\right)W_{\alpha\beta} - 3A_\beta W_{\alpha\beta\beta} + AW_{\alpha\beta\beta\beta} \end{bmatrix} \tag{J9}$$

$$(V^*)_\alpha = (V^\gamma)_\alpha - \frac{\gamma}{B}\left(-\frac{B_\alpha}{B}W_\beta + W_{\alpha\beta}\right) \tag{J10}$$

$$(V^*)_\beta = (V^\gamma)_\beta - \frac{\gamma}{B}\left(-\frac{B_\beta}{B}W_\beta + W_{\beta\beta}\right) \tag{J11}$$

$$(V^*)_{\alpha\alpha} = (V^\gamma)_{\alpha\alpha} - \frac{\gamma}{B^2}\left[\left(2\frac{B_\alpha^2}{B} - B_{\alpha\alpha}\right)W_\beta - 2B_\alpha W_{\alpha\beta} + BW_{\alpha\alpha\beta}\right] \tag{J12}$$

$$(V^*)_{\alpha\beta} = (V^\gamma)_{\alpha\beta} - \frac{\gamma}{B^2}\left[\left(2\frac{B_\alpha B_\beta}{B} - B_{\alpha\beta}\right)W_\beta - B_\beta W_{\alpha\beta} - B_\alpha W_{\beta\beta} + BW_{\alpha\beta\beta}\right] \tag{J13}$$

$$(V^*)_{\beta\beta} = (V^\gamma)_{\beta\beta} - \frac{\gamma}{B^2}\left[\left(2\frac{B_\beta^2}{B} - B_{\beta\beta}\right)W_\beta - 2B_\beta W_{\beta\beta} + BW_{\beta\beta\beta}\right] \tag{J14}$$

$$(V^*)_{\alpha\alpha\alpha} = (V^\gamma)_{\alpha\alpha\alpha} - \frac{\gamma}{B^2}\begin{bmatrix} \left(6\frac{B_\alpha B_{\alpha\alpha}}{B} - 6\frac{B_\alpha^3}{B^2} - B_{\alpha\alpha\alpha}\right)W_\beta + \cdots \\ \left(6\frac{B_\alpha^2}{B} - 3B_{\alpha\alpha}\right)W_{\alpha\beta} - 3B_\alpha W_{\alpha\alpha\beta} + BW_{\alpha\alpha\alpha\beta} \end{bmatrix} \tag{J15}$$

Journal of Vibration and Acoustics. Received December 07, 2017;
Accepted manuscript posted July 20, 2018. doi:10.1115/1.4040926

$$(V^*)_{\alpha\alpha\beta} = (V^\gamma)_{\alpha\alpha\beta} - \frac{\gamma}{B^2}\begin{bmatrix} \left(4\frac{B_\alpha B_{\alpha\beta}}{B} - 6\frac{B_\alpha^2 B_\beta}{B^2} + 2\frac{B_{\alpha\alpha}B_\beta}{B} - B_{\alpha\alpha\beta}\right)W_\beta + \cdots \\ \left(4\frac{B_\alpha B_\beta}{B} - 2B_{\alpha\beta}\right)W_{\alpha\beta} + \left(2\frac{B_\alpha^2}{B} - B_{\alpha\alpha}\right)W_{\beta\beta} - \cdots \\ 2B_\alpha W_{\alpha\beta\beta} - B_\beta W_{\alpha\alpha\beta} + BW_{\alpha\alpha\beta\beta} \end{bmatrix} \tag{J16}$$

$$(V^*)_{\alpha\beta\beta} = (V^\gamma)_{\alpha\beta\beta} - \frac{\gamma}{B^2}\begin{bmatrix} \left(4\frac{B_\beta B_{\alpha\beta}}{B} - 6\frac{B_\alpha B_\beta^2}{B^2} + 2\frac{B_{\beta\beta}B_\alpha}{B} - B_{\alpha\beta\beta}\right)W_\beta + \cdots \\ \left(2\frac{B_\beta^2}{B} - B_{\beta\beta}\right)W_{\alpha\beta} + \left(4\frac{B_\alpha B_\beta}{B} - 2B_{\alpha\beta}\right)W_{\beta\beta} - \cdots \\ 2B_\beta W_{\alpha\beta\beta} - B_\alpha W_{\beta\beta\beta} + BW_{\alpha\beta\beta\beta} \end{bmatrix} \tag{J17}$$

$$(V^*)_{\beta\beta\beta} = (V^\gamma)_{\beta\beta\beta} - \frac{\gamma}{B^2}\begin{bmatrix} \left(6\frac{B_\beta B_{\beta\beta}}{B} - 6\frac{B_\beta^3}{B^2} - B_{\beta\beta\beta}\right)W_\beta + \cdots \\ \left(6\frac{B_\beta^2}{B} - 3B_{\beta\beta}\right)W_{\beta\beta} - 3B_\beta W_{\beta\beta\beta} + BW_{\beta\beta\beta\beta} \end{bmatrix} \tag{J18}$$

Journal of Vibration and Acoustics. Received December 07, 2017;
Accepted manuscript posted July 20, 2018. doi:10.1115/1.4040926

Figures Caption

Figure S1 – Visualization of the tangent Projected Directions $\hat{\imath}$ and $\hat{\jmath}$ as seen from the viewing perspective. Note both vectors are still aligned with the x and y axis from that perspective even though these vectors are always tangent to the surface.

Figure S2 – Transformation Coefficients ρ_1 (a) and ψ_1(b) for the circular shell

Figure S3 – First row: displacement components $\overline{U}$ (a), $\overline{V}$ (b) and $\overline{W}$ (c) with respect to the standard unit vectors (i, j, k) of the circular shell. Second row: the in-plane displacements $\widehat{U}$ (d) and $\widehat{V}$ (e), and the out-of-plane displacement $\widehat{W}$ (f) with respect to the Projected Directions $\hat{\imath}$, $\hat{\jmath}$ and $\hat{k}$.

Figure S4 – Representation of the spatial derivatives along x and y. As an example, the input field $\widehat{V}$ (a) is shown, from which $\widehat{V}_x$(b) and $\widehat{V}_y$(c) can be derived.

Figure S5 – Change of coordinates by applying the chain rule. Here, the field $\widehat{V}_\alpha$ (e) is obtained by calculating the expression $\widehat{V}_x x_\alpha + \widehat{V}_y y_\alpha$ (Eq.(49)). Each of the quantities in the latter expression are shown above [$\widehat{V}_x$ (a), x_α (b), $\widehat{V}_y$ (d) and y_α (e)].

Figure S6 – Change of basis vectors representing the displacement components. In this example, the field $\widetilde{U}^{h/2}$ (e) is retrieved by using Eq.(50). The quantities $\widehat{U}$ (a), ρ_1 (b), $\widehat{V}$(c) and ψ_1(d) are found in the right-hand side of the equation.

Figure S7 – The in-plane displacement $\widetilde{U}$ (b) calculated from its value at the outer surface $\widetilde{U}^{h/2}$(a) by applying Eqs.(53, 55)

Figure S8 – First row: displacement components $\widetilde{U}$ (a), $\widetilde{V}$ (b) and $\widetilde{W}$ (c) of the triad $\mathbf{e}_1$, $\mathbf{e}_2$ and $\mathbf{e}_3$. Second row: 1st order spatial derivatives of $\widetilde{U}$, $\widetilde{V}$ and $\widetilde{W}$ with respect to α, i.e., $\widetilde{U}_\alpha$ (d), $\widetilde{V}_\alpha$ (e) and $\widetilde{W}_\alpha$ (f). Third row: spatial derivatives of the corresponding displacements with respect to β, i.e., $\widetilde{U}_\beta$ (g), $\widetilde{V}_\beta$ (h) and $\widetilde{W}_\beta$ (i).

Journal of Vibration and Acoustics. Received December 07, 2017;
Accepted manuscript posted July 20, 2018. doi:10.1115/1.4040926

Figures List

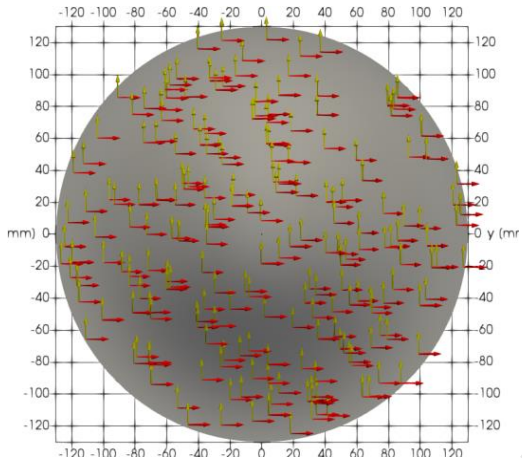

Figure S1 – Visualization of the tangent Projected Directions $\hat{\imath}$ and $\hat{\jmath}$ as seen from the viewing perspective. Note both vectors are still aligned with the x and y axis from that perspective even though these vectors are always tangent to the surface.

Journal of Vibration and Acoustics. Received December 07, 2017;
Accepted manuscript posted July 20, 2018. doi:10.1115/1.4040926

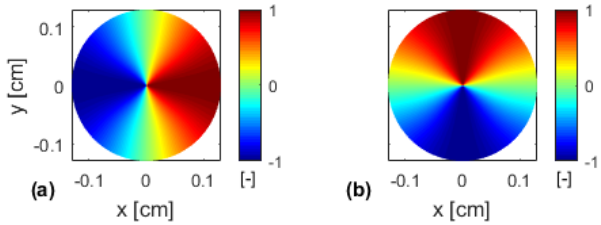

Figure S2 – Transformation Coefficients ρ_1 (a) and ψ_1(b) for the circular shell

Journal of Vibration and Acoustics. Received December 07, 2017;
Accepted manuscript posted July 20, 2018. doi:10.1115/1.4040926

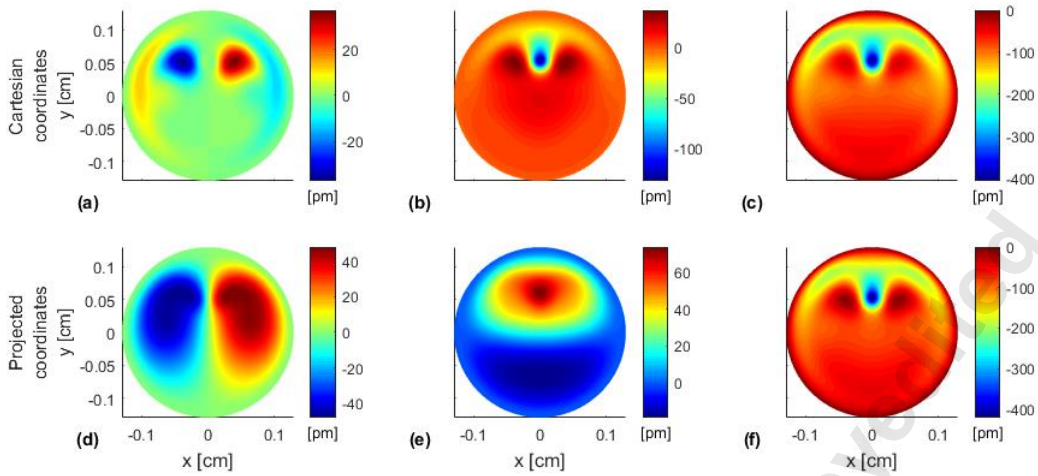

Figure S3 – First row: displacement components $\overline{U}$ (a), $\overline{V}$ (b) and $\overline{W}$ (c) with respect to the standard unit vectors $(\mathbf{i}, \mathbf{j}, \mathbf{k})$ of the circular shell. Second row: the in-plane displacements $\widehat{U}$ (d) and $\widehat{V}$ (e), and the out-of-plane displacement $\widehat{W}$ (f) with respect to the Projected Directions $\hat{\mathbf{i}}$, $\hat{\mathbf{j}}$ and $\hat{\mathbf{k}}$.

Journal of Vibration and Acoustics. Received December 07, 2017;
Accepted manuscript posted July 20, 2018. doi:10.1115/1.4040926

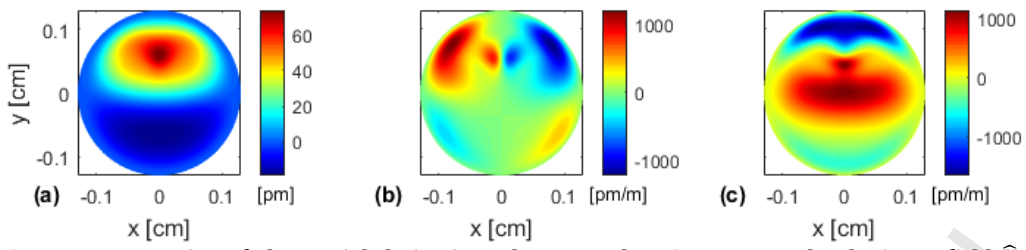

Figure S4 – Representation of the spatial derivatives along x and y. As an example, the input field $\hat{V}$ (a) is shown, from which $\hat{V}_x$(b) and $\hat{V}_y$(c) can be derived.

Journal of Vibration and Acoustics. Received December 07, 2017;
Accepted manuscript posted July 20, 2018. doi:10.1115/1.4040926

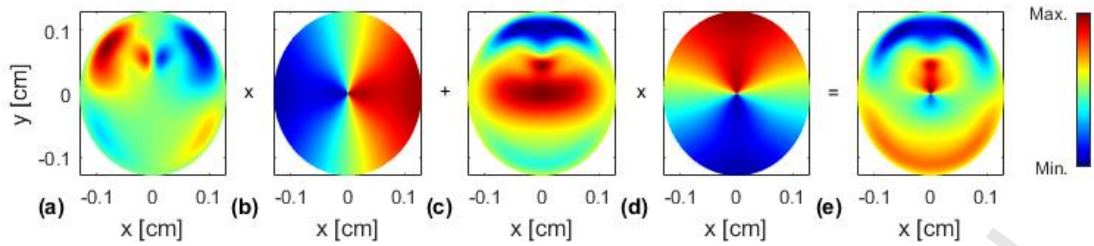

Figure S5 – Change of coordinates by applying the chain rule. Here, the field $\widehat{V}_\alpha$ (e) is obtained by calculating the expression $\widehat{V}_x x_\alpha + \widehat{V}_y y_\alpha$ (Eq.(49)). Each of the quantities in the latter expression are shown above [$\widehat{V}_x$ (a), x_α (b), $\widehat{V}_y$ (d) and y_α (e)].

Journal of Vibration and Acoustics. Received December 07, 2017;
Accepted manuscript posted July 20, 2018. doi:10.1115/1.4040926

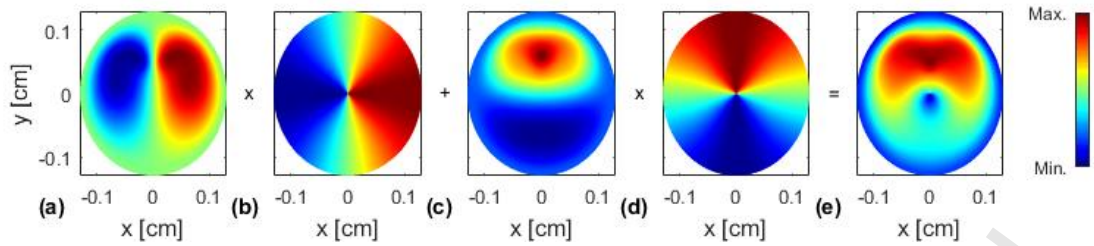

Figure S6 – Change of basis vectors representing the displacement components. In this example, the field $\widetilde{U}^{h/2}$ (e) is retrieved by using Eq.(50). The quantities $\widehat{U}$ (a), ρ_1 (b), $\widehat{V}$(c) and ψ_1(d) are found in the right-hand side of the equation.

Journal of Vibration and Acoustics. Received December 07, 2017;
Accepted manuscript posted July 20, 2018. doi:10.1115/1.4040926

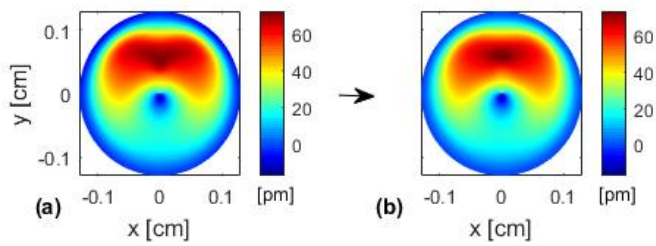

Figure S7 – The in-plane displacement $\widetilde{U}$ (b) calculated from its value at the outer surface $\widetilde{U}^{h/2}$(a) by applying Eqs.(53, 55)

Journal of Vibration and Acoustics. Received December 07, 2017;
Accepted manuscript posted July 20, 2018. doi:10.1115/1.4040926

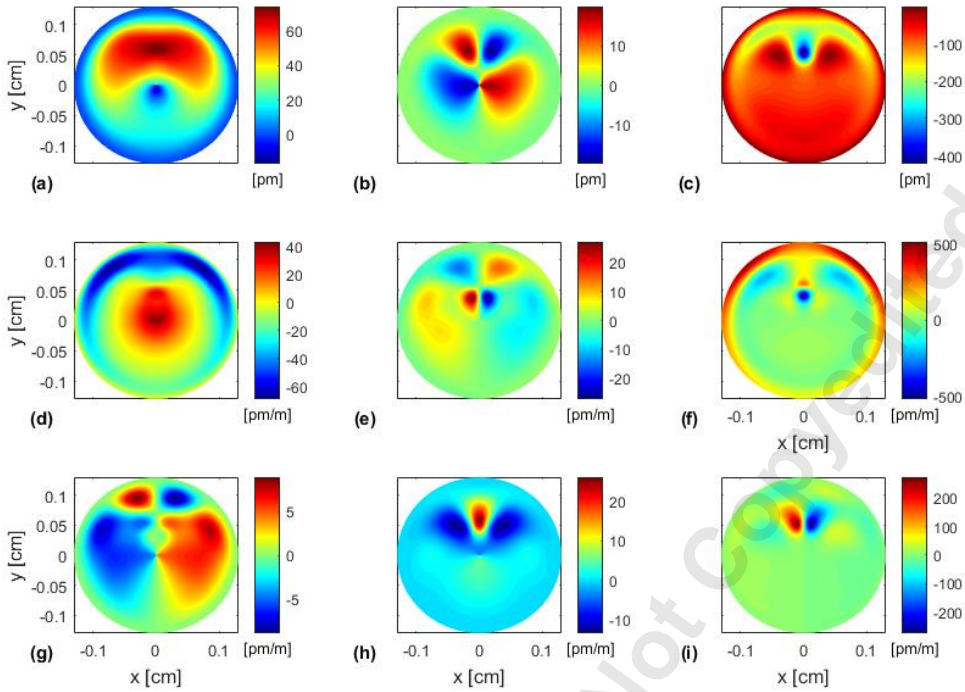

Figure S8 – First row: displacement components $\widetilde{U}$ (a), $\widetilde{V}$ (b) and $\widetilde{W}$ (c) of the triad $\mathbf{e}_1$, $\mathbf{e}_2$ and $\mathbf{e}_3$. Second row: 1st order spatial derivatives of $\widetilde{U}$, $\widetilde{V}$ and $\widetilde{W}$ with respect to α, i.e., $\widetilde{U}_\alpha$ (d), $\widetilde{V}_\alpha$ (e) and $\widetilde{W}_\alpha$ (f). Third row: spatial derivatives of the corresponding displacements with respect to β, i.e., $\widetilde{U}_\beta$ (g), $\widetilde{V}_\beta$ (h) and $\widetilde{W}_\beta$ (i).